Comparison of gene set scoring methods for reproducible evaluation of multiple tuberculosis gene signatures

Xutao Wang, M.Sc[1,2]; Arthur VanValkenberg, Ph.D.[2], Aubrey R. Odom-Mabey[2], Jerrold J. Ellner, M.D.[3]; Natasha S. Hochberg, M.D., M.P.H.[4,5]; Padmini Salgame, Ph.D[3]; Prasad Patil, Ph.D[1,*]; W. Evan Johnson, Ph.D[6,*]

Institutions:

[1]Department of Biostatistics, Boston University, Boston, MA, USA

[2]Division of Computational Biomedicine and Bioinformatics Program, Boston University, Boston, MA, USA

[3]Department of Medicine, Center for Emerging Pathogens, Rutgers New Jersey Medical School, Newark, NJ, USA

[4]Boston Medical Center, Boston, MA, USA

[5]Section of Infectious Diseases, Boston University School of Medicine, Boston, MA, USA

[6]Division of Infectious Disease, Center for Data Science, Rutgers New Jersey Medical School, Newark, NJ, USA

* WEJ and PP are co-senior authors

Corresponding Author: W. Evan Johnson, Ph.D., New Jersey Medical School, 225 Warren Street 450G, Newark, NJ, USA 07103. Email: w.evan.johnson@rutgers.edu

Authors Contribution: WEJ and PP conceived the study. XW conducted the comparisons and analysis of TB signatures and generated the figures. All authors contributed to the study design and guided the interpretation of the results. XW, PP and WEJ wrote the manuscript and generated figures and results. All authors read and approved the final manuscript.

Funding Sources: This work was supported by funds from the NIH (R01GM127430 and R21AI154387)

Keywords: Tuberculosis, genet set scoring methods, gene signatures, reproducibility

ABSTRACT

Rationale: Many blood-based transcriptional gene signatures for tuberculosis (TB) have been developed with potential use to diagnose disease, predict risk of progression from infection to disease, and monitor TB treatment outcomes. However, an unresolved issue is whether gene set enrichment analysis (GSEA) of the signature transcripts alone is sufficient for prediction and differentiation, or whether it is necessary to use the original statistical model created when the signature was derived. Intra-method comparison is complicated by the unavailability of original training data, missing details about the original trained model, and inadequate publicly-available software tools or source code implementing models. To facilitate these signatures' replicability and appropriate utilization in TB research, comprehensive comparisons between gene set scoring methods with cross-data validation of original model implementations are needed.

Objectives: We compared the performance of 19 TB gene signatures across 24 transcriptomic datasets using both re-rebuilt original models and gene set scoring methods to evaluate whether gene set scoring is a reasonable proxy to the performance of the original trained model. We have provided an open-access software implementation of the original models for all 19 signatures for future use.

Methods: We considered existing gene set scoring and machine learning methods, including ssGSEA, GSVA, PLAGE, Singscore, and Zscore, as alternative approaches to profile gene signature performance. The sample-size-weighted mean area under the curve (AUC) value was computed to measure each signature's performance across datasets. Correlation analysis and Wilcoxon paired tests were used to analyze the performance of enrichment methods with the original models.

Measurement and Main Results: For many signatures, the predictions from gene set scoring methods were highly correlated and statistically equivalent to the results given by the original diagnostic models. PLAGE outperformed all other gene scoring methods.

In some cases, PLAGE outperformed the original models when considering signatures' weighted mean AUC values and the AUC results within individual studies.

Conclusion: Gene set enrichment scoring of existing blood-based biomarker gene sets can distinguish patients with active TB disease from latent TB infection and other clinical conditions with equivalent or improved accuracy compared to the original methods and models. These data justify using gene set scoring methods of published TB gene signatures for predicting TB risk and treatment outcomes, especially when original models are difficult to apply or implement.

INTRODUCTION

Prior to the COVID-19 pandemic, tuberculosis (TB) was the leading infectious cause of death worldwide (1, 2). Approximately 10 million people developed TB, and 1.4 million died from the disease (1). Current diagnostic tests for TB disease include sputum acid-fast bacilli (AFB) smear microscopy, rapid molecular tests, and culture-based technologies (1). With the advent and widespread availability of nucleic acid amplification tests (Xpert MTB/RIF), most cases of pulmonary TB can be diagnosed quickly and accurately. Paucibacillary TB diagnosis (smear-negative pulmonary, extrapulmonary, and pediatric TB) (3–6) and predicting treatment success/failure remain difficult challenges. Furthermore, there are gaps in identifying individuals with quiescent or percolating disease, and utilizing non-sputum-based technologies would facilitate diagnosis for individuals unable to produce sputum (e.g., children). There is therefore an urgent need for additional technologies that ensure high-quality, timely, effective testing for people living with TB (1, 7).

Over the last ten years, multiple blood-based biomarkers using gene expression profiles have been developed for TB. These signatures can distinguish active TB disease from latent TB infection (LTBI) (8, 9), distinguish TB from other diseases (OD) (10–12), predict progression from LTBI to active TB (13, 14), and assess treatment response (15). These or other signatures may potentially meet target product profiles (TPP) proposed by the World Health Organization (WHO) for point-of-care (POC) testing, since some studies have shown that perturbation in the gene expression profile occurs prior to sputum conversion (13, 14, 16, 17). Blood-based signatures could also identify individuals for additional diagnostics or LTBI treatment. However, more research must be done to establish the efficacy and reproducibility of using blood-based signatures in the field, as shown by the CORTIS trial (18).

The common approach to building a gene signature is to identify a *gene set*, a subset of the thousands of genes whose expression is measured for a patient cohort, using a combination of domain knowledge and data-driven feature selection methods. The gene set is then used to train a gene signature using a *prediction algorithm* such as

101 regression or some other machine learning approaches for deciding how to turn gene
102 expression measurements into an outcome prediction. Typically, biomarkers are *trained*
103 using one subset of data and then finalized or *fixed* before being applied for prediction
104 in new samples and cohorts. However, in the case of existing TB signatures, the
105 *replicability* of these biomarkers is inadequate, meaning that many of the original
106 publications did not give enough detail to replicate the published models. In addition,
107 nearly all of these publications failed to provide usable code to rerun the published
108 model on the study data—let alone apply the models to new datasets. Some of these
109 original models further lacked *reproducibility* of the performance and accuracy of TB
110 gene signatures—meaning that the signatures were *overfit* and thus experienced
111 significant reductions in performance in later observations compared to the training set
112 (10, 19, 20). Many factors likely contribute to this phenomenon, including overfitting to
113 encodes in the training data, incomplete validation of the biomarker, differences in study
114 population demographics or comorbidities, and possible inconsistencies due to
115 differences in the platforms used to measure gene expression (37, 46).
116
117 Several research teams have attempted to address issues of reproducibility in TB gene
118 expression biomarker research, either by rebuilding the original classification models (7,
119 19) or by using methods such as gene set enrichment analysis (GSEA) in place of the
120 original models (21). For example, Warsinske et al. (19) reconstructed the original
121 models for 16 TB gene signatures and compared gene signature accuracy in the
122 contexts of TB diagnostics and progression to disease. For some of their biomarkers,
123 the discovery dataset(s) used to train the gene signatures were unavailable, or the
124 proposed diagnostic models comprised the gene signatures were difficult to reproduce.
125 Other challenges included limited information about data preprocessing and
126 hyperparameter values used to build the model (22–24). Despite clear documentation of
127 their reconstruction of original models, Warsinske et al. (19) did not publish software
128 code for their work from scratch to use the biomarkers from their comparisons.
129
130 As a result of this deficit in replicability, we have endeavored to fill this gap. Our team
131 has recently developed and released the open-source TBSignatureProfiler software

132 toolkit, which provides a compilation of TB gene sets used from published biomarkers
133 and provides methods (21) to evaluate the performance of existing TB gene sets on
134 new datasets via the application of various scoring algorithms (25) (e.g., GSVA,
135 ssGSEA, PLAGE). However, while alternative methods, such as gene set scoring are
136 simpler to use compared to the original models, these methods have not been
137 established as reasonable approximations or alternatives to original model
138 performance.
139
140 To address the issues of reproducibility in reconstructing the discovery set, our study
141 uniformly evaluated the performance of 19 TB gene signatures across 24 datasets
142 using both original models and gene set scoring methods through the
143 TBSignatureProfiler platform. We systematically compared our results to previous
144 research (19) to the signature's ability to distinguish patients with active TB from other
145 clinical conditions. Our results illustrated that gene set scoring methods are effective
146 computational tools for profiling the performance of TB gene signatures and produced
147 similar accuracy compared to the original model, demonstrating alternative, accessible
148 ways to profile existing TB gene signatures. We also sought to facilitate the replicability
149 of TB gene signatures' application and comparative analysis. We therefore curated the
150 TB transcriptomic datasets used in this study and included the corresponding discovery
151 model for each gene signature in the TBSignatureProfiler R package, enabling the
152 reproducibility of all results.

153 **METHODS**

154 **Gene signatures and original diagnostic models used for comparison**

155 Nineteen existing TB gene signatures were selected for this study primarily based on
156 the results of Warsinske *et al*. (Table 1) (10, 12–14, 22–24, 26–32) to make a fair
157 comparison for the performance of these signatures. Sixteen gene signatures were
158 trained to predict active TB versus other clinical conditions. Three additional gene
159 signatures that predict progression from LTBI to active TB disease, Zak_RISK_16 (14),
160 Suliman_RISK_4 (13), and Leong_RISK_29 (32), were also included. Twenty-four
161 datasets (9–12, 16, 21, 27–29, 31, 33–48) that include subjects with active TB and other
162 clinical conditions have been selected for evaluation. These datasets were selected in
163 alignment with Warsinske *et al*. to systematically compare different gene scoring
164 methods and the original models (19). Twenty of these datasets were from microarray
165 studies; the other four consisted of RNA-sequencing data. A detailed description of the
166 transcriptomic studies included in this study can be found in the Supplementary
167 Material.
168
169 The reconstruction of each signature's original model followed the guidelines given by
170 Warsinske et al. (20), who reconstructed these models based on information from each
171 of the signature's original publications. Two training methods were used for TB gene
172 signature discovery: model-based and score-based approaches. The model-based
173 approaches use machine learning algorithms such as support vector machines (33) or
174 random forests (49) to reconstruct the biomarker's original model. The score-based
175 approaches primarily rely on the difference of sums or arithmetic means between the
176 upregulated genes and the downregulated genes within the gene set and therefore do
177 not require model retraining. Six of the 19 identified gene signatures used score-based
178 methods to distinguish active TB patients from other clinical conditions (Table 1). The
179 reconstructed models were validated against the performance reported in the original
180 publication using the AUC metric. To evaluate a biomarker's ability to identify patients
181 with active TB, the associated model was applied across the 24 curated transcriptomic
182 studies.

183 **Gene set scoring methods**

184 We used single sample GSEA (ssGSEA) (50), Gene Set Variation Analysis (GSVA)
185 (35), Pathway level analysis of gene expression (PLAGE) (51), Zscore (52), and
186 Singscore (unidirectional and bidirectional versions) (50, 53) to evaluate the accuracy of
187 TB gene signatures across 24 studies. Please see the Discussion section for a more
188 detailed comparison of these five gene set scoring methods. The evaluation of distinct
189 gene signatures using different gene set scoring methods and its original model was
190 performed by the runTBSigProfiler function from the TBSignatureProfiler R package
191 (38).
192

193 **Gene signature splitting strategy**

194 Some gene set scoring methods, including GSVA, ssGSEA, and Singscore, rank a
195 signature's genes against other genes in the dataset. Thus, gene sets with both
196 upregulated and downregulated genes do not usually score well with these methods—
197 they effectively counteract each other in the score computation. Most of the 19
198 signatures contain genes expressed strongly in both directions; thus, we proposed a
199 'signature splitting' strategy for gene signatures with equal to or more than ten genes to
200 overcome this limitation. Gene signatures with less than ten genes were excluded here
201 as their upregulated or downregulated gene subset was either empty or only contained
202 one gene. In such cases, signature splitting would have a decreased effect on these
203 gene sets compared to a large set.
204

205 For the ssGSEA and GSVA methods, we evaluated each signature's performance using
206 only the upregulated or the downregulated subsets of genes within the gene sets. For
207 gene signatures that did not require reconstruction of the training model, the
208 upregulated and downregulated genes were usually provided by the original publication.
209 If unavailable in the original publication, the upregulated or the downregulated genes
210 were identified by performing differential expression analysis on the datasets from which
211 the associated biomarkers were derived using the R package DESeq2 (54) for RNA-seq
212 data and limma (55) for microarray data. For the bidirectional implementation of
213 Singscore, we used the simpleScore function from the singscore R package (53) to

214 algorithmically combine the disease score for the upregulated and downregulated
215 genes.
216
217 **Imputation of missing genes and removal of batch effects**
218 Occasionally, various genes within gene sets were missing across transcriptomic
219 studies, mainly due to the inconsistent gene coverage across platforms or different
220 versions of the gene symbol naming systems across different sequencing platforms.
221 This might affect a biomarker's predictive accuracy in some datasets and across
222 biomarker methods. Two steps were taken to mitigate this issue. First, we updated gene
223 symbols for gene signatures and candidate datasets using the HGNChelper R package
224 (56) to reduce gene misidentification during the training and validation process. More
225 details on the matching of probe ID to gene symbol and missing gene information within
226 each dataset can be found in the Supplementary Material. Second, a k-nearest
227 neighbors (KNN) algorithm was applied to impute the missing gene expression values
228 based on the signature's discovery dataset(s) (57). This procedure may elicit potential
229 bias problems when large portions of genes within a signature are missing in some
230 datasets. To make a fair comparison, we applied this imputation procedure to all
231 biomarkers that used model-based diagnostic approaches across independent
232 datasets. Functionality *reference ComBat* (58, 59) was used to make generalized
233 comparisons of signatures across the independent studies. *reference ComBat* removes
234 batch effects between the training datasets and the testing datasets without changing
235 the reference dataset's gene expression values. With this functionality, the biomarker's
236 original model does not have to be retrained whenever the batch correction is
237 performed or when the model is applied to a new dataset, increasing efficiency when
238 evaluating biomarkers with model-based approaches.
239
240 **Statistical Evaluation of Model Performance**
241 The AUC value corresponding to sample scores against disease subtypes for each TB
242 gene signature was calculated for each dataset. The sample-size-weighted mean AUC
243 (weighted AUCs) was used to assess the overall performance of each gene set across
244 independent studies while excluding the discovery dataset(s) used to train the

245 corresponding signature (44). AUC results were calculated with the R package ROCit
246 (60) compute estimates. Each signature's 95% confidence interval for the weighted
247 mean AUC value was calculated using the bootstrap method with 10,000 bootstrap
248 resamples. The Wilcoxon paired test was applied to test whether AUCs given by
249 different methods were significantly different from each other.
250

251 **Evaluating biomarker performance based on original models**

252 The original models were inputted into the TBSignatureProfiler (45) platform, which
253 provides a computational profiling platform that allows researchers to evaluate multiple
254 TB gene signatures. In addition to the original models, users can access other scoring
255 methods and gene sets in the TBSignatureProfiler. The TBSignatureProfiler was used
256 to conduct all the analyses for this work, and the package can be downloaded from
257 GitHub (https://github.com/compbiomed/TBSignatureProfiler) or Bioconductor
258 (http://www.bioconductor.org/packages/release/bioc/html/TBSignatureProfiler.html).
259 Code for the analyses from this paper can be found at: https://github.com/xutao-
260 wang/Comparison-of-existing-tuberculosis-gene-signatures.
261

262 **Comparing the performance of gene set scoring methods with original models**

263 We noticed that there are several studies (i.e. GSE81746, GSE107331, GSE29536 etc.)
264 with a small sample sizes ($n < 40$) which only consisted of healthy controls (HCs) and
265 subjects with active TB. For these studies, most was generalizable to gene signatures
266 that could distinguish patients with active TB phenotype with high predictive accuracy;
267 however, such performance could not be generalized toward large populations or to
268 cohorts with heterogeneous disease types including LTBI. To produce a fair comparison
269 of gene signatures' performance using gene set scoring methods and their original
270 models, for each profiling method (including both gene set scoring methods and original
271 models) we selected datasets with a sample size greater than 40 and AUC estimates
272 greater than 0.80 across all TB biomarkers simultaneously excluding the corresponding
273 training study for each biomarker.
274

Several metrics were used to compare the performance of gene signatures as assessed by different gene set scoring methods and their original models. For each TB gene signature, the Spearman's rank correlation (ρ) was computed to measure the strength of association of the prediction scores from a signature's original model and the different gene set scoring methods. We then summarized correlation results, computing the weighted Spearman's rank correlation (ρ_w), based on equation 1.

$$\rho_w = \frac{\sum_{i=1}^{k} \rho_i * n_i}{\sum_{i=1}^{k} n_i} \tag{1}$$

Moreover, the absolute AUC difference ($|\Delta AUC|$) between the original model and various gene set scoring methods were computed as shown in equation 2.1 for each selected dataset, with the weighted absolute AUC difference $|\Delta AUC|_w$ representing the overall distribution pattern across all selected studies (equation 2.2). Additionally, the Szymkiewicz–Simpson coefficient (61) or overlap coefficient (oc) as shown by equation (3), was applied to evaluate the similarity of studies based on the results given by each of the gene set scoring method and original model for all gene signatures.

$$|\Delta AUC_i| = \left|AUC_{GSEA,i} - AUC_{original\ model,i}\right| \tag{2.1}$$

$$|\Delta AUC|_w = \frac{\sum_{i=1}^{k} |\Delta AUC_i| * n_i}{\sum_{i=1}^{k} n_i} \tag{2.2}$$

$$overlap\ coefficient = \frac{\#\ of\ common\ datasets}{min\left(n_{GSEA}, n_{original\ model}\right)} \tag{3}$$

297 **RESULTS**

298 **Evaluation of discovery studies using training models from original publications**

299 The list of signatures and information on their respective training data are presented in
300 Table 1, along with AUC values from their originating publication, Warsinske *et al*., and
301 our results. The AUC values for our reconstructed models were nearly identical to the
302 results of the original publications, suggesting that the training models were accurately
303 reconstructed. Several gene signatures including Sweeney_OD_3, Maertzdorf_15,
304 Leong_24, Kaforou_27, Anderson_42, and Berry_393, when evaluated by ssGSEA, had
305 estimated AUC values above 0.9 (Table S1). These results suggest that ssGSEA is a
306 comparable signature profiling method, producing accurate results for some TB
307 signatures in differentiating the TB disease states (active TB vs. LTBI, HCs, or OD)
308 even if the evaluation studies were the signature's discovery datasets.
309

310 **Performance of original models and gene set scoring methods for active TB**
311 **versus non-active TB**

312 Figure 1 shows the AUC distribution of 24 independent TB studies across 19 TB gene
313 signatures based on the results from their original models. 13 of 16 signatures had
314 AUCs greater than 0.9 from their discovery dataset(s) (Figure 1). Each TB signature's
315 original model was applied across all the datasets, and their performance varied greatly
316 on a study-by-study basis (Figure 1). Notably, the Kaforou_OD_53, Kaforou_27,
317 Maertzdorf_15, and Sweeney_OD_3 signatures had consistently high AUC values
318 across different studies, with weighted AUCs of 0.83 for Kaforou_OD_53, 0.81 for
319 Kaforou_27, 0.82 for Maertzdorf_15, and 0.81 for Sweeney_OD_3 (Table 2). In
320 contrast, the performance of some signatures, such as Verhagen_10, was mixed across
321 studies (Figure 1). Verhagen_10 had a weighted mean AUC of 0.61 (Table 2),
322 performing well in some datasets (>0.9 AUC in GSE81746, GSE41055, and GSE29536)
323 but with poor performance in most of the remaining studies (<0.65 AUC in 16 out of 24
324 studies; Figure 1). Noted that Zak_RISK_16, Suliman_RISK_4, and
325 Leong_PREDICT_29 also performed poorly in these comparisons, but these are
326 signatures of disease progression (Figure 1).

Table 2 shows the weighted AUCs for each gene signature as computed using their corresponding original model and five different gene set scoring methods. In this table, AUC values in red denote results from our reimplemented models and gene set scoring methods that outperformed the original model with differences greater than 0.05 units. Values in blue represent cases where AUC values from the original model outperformed other methods the methods by more than 0.05 units. The 0.05 threshold was chosen mainly for visualization purposes, which suggested that there was a noticeable difference in the weighted AUCs given by two different methods.

16 of 19 gene signatures had reimplemented weighted AUCs within 0.05 units compared to Warsinske *et al*. (Table 2). However, our reimplemented models for Verhagen_10 and Anderson_OD_51 outperformed the results from Warsinske *et al*., and our original model for Jacobsen_3 underperformed compared to Warsinske *et al*. (Table 2). The weighted AUCs for Anderson_OD_51 computed by gene scoring methods surpassed that of its original model but not the results given by ssGSEA, although none of the results were statistically significant after adjusting for multiple testing (p-value > 0.01; Table 2). For Berry_393, the weighted AUCs computed from its original model underperformed all the five gene scoring methods; specifically, the PLAGE AUC was 0.79 (95% CI: 0.75–0.84), which was significantly higher (p-value <= 0.01) than that of the original model which had an AUC of 0.70 (0.66–0.74). Results from Zak_RISK_16 given by its original model also underperformed five gene scoring methods, and all the superior weighted AUCs were significant (p-value <= 1e-04) (Table 2). Additionally, the performance of each gene signature across individual datasets using five gene set scoring methods was presented in Figure S1A-E.

Figure 2A shows the weighted mean AUC difference between the original model and the corresponding five gene scoring methods across all gene sets. The outperformance of the weighted AUCs given by PLAGE was consistent in most of the gene signatures asides from Sambarey_HIV_10 and Anderson_42. The accompanying Wilcoxon signed-rank test results indicated that the results from PLAGE were significantly different from

358 the results of the original models (p-value <= 0.01), whereas the results from the
359 remaining four gene scoring methods were statistically equivalent when compared to
360 the weighted AUCs given by the original model (p-value > 0.05; Figure 2A).
361
362 ***Accounting for gene expression direction***

363 Table 3 shows the weighted mean AUCs from ssGSEA and GSVA after splitting the
364 genes into upregulated or downregulated subsets, along with the Singscore bidirectional
365 scoring results. There was significant improvements in the weighted AUCs for the
366 upregulated subsets of Berry_OD_86 based on the ssGSEA (AUC = 0.78; 95% CI:
367 0.75–0.82) and GSVA (AUC = 0.80; 95% CI: 0.76–0.84) results when compared to its
368 original models (p-value <= 1e-04 for both methods; Table 3). Similar improvement was
369 observed when using ssGSEA and GSVA for the upregulated subsets of Berry_393 (p-
370 value <= 0.01 for both methods). Interestingly, Anderson_OD_51 is the only gene
371 signature for which the weighted AUCs from GSVA (upregulated subsets: AUC = 0.81,
372 95% CI: 0.78-0.84; p-value = 0.03; downregulated subsets AUC = 0.77, 95% CI: 0.71-
373 0.82; p-value = 0.04) outperformed its original model (Table 3). Lastly, the performance
374 of Berry_OD_86 and Berry_393 given by Singscore bidirectional scoring also
375 outperformed their original models (p-value <= 1e-3 for both gene sets; Table 3). Most
376 gene signatures had similar results when using the unidirectional and bidirectional
377 versions of Singscore, although Sambarey_HIV_10 and Anderson_OD_51 showed
378 significantly lower weighted AUCs using Singscore bidirectional scoring (p-value < 0.01
379 for both gene sets; Tables 2 and 3).
380

381 Figure 2B illustrates the weighted mean AUC differences between each gene scoring
382 method and original models across gene signatures. Again, the Wilcoxon signed-rank
383 test suggests that the weighted mean AUC results from all methods were statistically
384 equivalent (p-value > 0.05) to the results given by the original model, except for the
385 results computed from the signatures' downregulated subset using ssGSEA (p-value =
386 0.036; Figure 2B). Additionally, Figure S2A-C shows the AUC distribution for the
387 up/down-regulated subset of each qualified gene signature across all datasets using the
388 gene set scoring methods ssGSEA, GSVA, and Singscore bidirectional scoring.

Finally, ridge plots displayed the AUC distribution across 24 studies using original models and all the five gene set scoring methods (Figure S3A-C). The gene signatures were ranked in increasing order based on their median AUC values over the individual training dataset used by the given original model. Signatures including Kaforou_27, Kaforou_OD_53, and Sambarey_HIV_10 had statistically equivalent AUC distributions for results obtained from their respective original models, PLAGE, and ssGSEA with the upregulated subset (Kaforou_27 p-value = 0.54, Kaforou_OD_53 p-value = 0.93, Sambarey_HIV_10 p-value = 0.88; Figure S3A).

Gene set scoring methods versus original models

Figure S4A-E shows the performance of 19 gene signatures after selection, as based on the criteria described in the methods section. Each point represents a single study; the y-axis gives Spearman's rank correlation of the predicted scores for the original model and respective gene set scoring method, and the x-axis gives the AUC difference between the results given by two different methods. As expected, Verhagen_10 had poor performance when evaluated using its original model, Zscore, and Singscore. None of the studies had AUCs greater than 0.8 after selection (Figure S4A-E). GSE101705 was the only study selected, but it showed a distinct prediction pattern given by ssGSEA/GSVA when compared to its original model (0.18 <= $|\Delta AUC|$ <= 0.21; 0.35 <= ρ <= 0.57). Similar mediocre performance was observed for Suliman_RISK_4, where GSE107994 was the only study selected by ssGSEA and its original model ($|\Delta AUC|$ = 0.061; ρ = 0.7; Figure S4A), and no studies were selected using GSVA and Zscore (Figure S4C-D). In addition, no studies had AUCs greater than 0.8 for Leong_RISK_29 when evaluated using ssGSEA, GSVA, and Zscore (Figure S4A; Figure S4C-D)

ssGSEA vs. Original Model

Kaforou_27, Maertzdorf_15, and Sweeney_OD_3 showed high diagnostic accuracy in similar studies (oc for Kaforou_27 and Maertzdorf_15: = 1.00, oc for Sweeney_OD_3: = 0.86) with small AUC differences (p-value > 0.28 for three gene sets) given by ssGSEA

and their original models. Significantly positive Spearman's rank correlations of the predicted scores were shown for Kaforou_27 (ρ_w = 0.78) and Sweeney_OD_3 (ρ_w = 0.86), and significantly negative correlations were produced for Maertzdorf_15 (ρ_w = -0.81; p-value <= 1e-04 for three signatures; Figure S4A). Although more studies with high AUCs were selected for Anderson_OD_51, Berry_393, Berry_OD_86, Bloom_OD_144, Leong_24, and Zak_RISK_16 using ssGSEA, results from these six signatures showed distinct predicted results when compared to their original models (0.032 <= ρ_w <= 0.60; $|\Delta AUC|_w$ > 0.050; Figure S4A). Conversely, more datasets were selected for Kaforou_OD_44, Kaforou_OD_53, LauxdaCosta_OD_3, and Maertzdorf_4 based on the results from these signatures' original models (0.070 <= ρ_w <= 0.72, $|\Delta AUC|_w$ > 0.050; Figure S4A).

PLAGE vs. Original Model

For gene sets Kaforou_27, Kaforou_OD_53, LauxdaCosta_OD_3, Maertzdorf_4, and Maertzdorf_15, PLAGE results were nearly equivalent to the results from their original models (Figure S4B). The study overlap coefficient was 1.00 for all five gene signatures, asides from Kaforou_OD_53, with an AUC value of 0.85 (Figure S4B). Specifically, Kaforou_27, Kaforou_OD_53, and LauxdaCosta_OD_3 had significantly negative Spearman's rank correlations for the predicted results given by two methods (-0.92 < ρ_w < -0.82; p-value < 1e-04 for all three gene sets), with an absolute weighted AUC difference less than 0.030 for all three gene sets. Two Maertzdorf signatures had strong positive Spearman's rank correlations of the prediction scores and small AUC differences (p-value for Maertzdorf_4: = 0.06, p-value for Maertzdorf_15: = 0.02), with ρ_w of 0.88 for Maertzdorf_4 and of 0.94 for Maertzdorf_15 (p-value < 1e-05; Figure S4B). Asides from these gene sets, 11 of 14 signatures (excluding Anderson_42, Kaforou_OD_44, and Sambarey_HIV_10) had a higher number of studies with high AUCs selected by PLAGE but showed large absolute AUC differences ($|\Delta AUC|_w$ > 0.080) and weak to moderate correlations (-0.68 <= ρ_w<= 0.62) of the profiling scores when compared to the results from their original methods (Figure S4B).

GSVA vs. Original Model

When comparing the results given by GSVA and signatures' original models, more studies were selected for Anderson_OD_51, Berry_393, Berry_OD_86, Bloom_OD_144, and Zak_RISK_16 with weighted absolute AUC differences all greater than 0.050 and weak Spearman's rank correlation (0.11 <= ρ_w <= 0.47) of the predicted scores (Figure S4C). Similar to that of ssGSEA, the resulting scores from Maertzdorf_15 (ρ_w = -0.78, $|\Delta AUC|_w$ = 0.043) and Maertzdorf_4 (ρ_w = -0.63, $|\Delta AUC|_w$ = 0.051) were negatively correlated with the results from the signatures' original model, with a study overlap coefficient of 1.00 for both gene signatures (Figure S4C).

Zscore vs. Original Model

The performance of gene signatures using Zscore was similar to GSVA, for which more datasets were selected for Anderson_OD_51, Berry_393, Berry_OD_86, Bloom_OD_144, and Zak_RISK_16. However, a distinct prediction pattern was visible when comparing these to their original methods (-0.0037 <= ρ_w <= 0.65, $|\Delta AUC|_w$ > 0.05 for all five gene sets; Figure S4D). Similar to the results from ssGSEA and GSVA, Maertzdorf_15 (ρ_w = -0.85, $|\Delta AUC|_w$ = 0.044) and Maertzdorf_4 (ρ_w = -0.74, $|\Delta AUC|_w$ = 0.084) had negatively correlated prediction scores given using Zscore and their respective original models (Figure S4D).

Singscore unidirectional scoring vs. Original Model

Although more studies with high AUCs were selected when assessing Anderson_OD_51, Berry_393, Berry_OD_86, Bloom_OD_144, and Zak_RISK_16 with Singscore unidirectional scoring, results from these signatures had weak to moderate weighted Spearman's rank correlation (0.16 <= ρ_w <= 0.55) and a large AUC difference ($|\Delta AUC|_w$ >= 0.11 for all five gene sets; Figure S4E). Conversely, no datasets with high AUCs were selected for Anderson_42 (ρ_w = -0.23, $|\Delta AUC|_w$ = 0.26) based on results given by Singscore unidirectional scoring. Sweeney_OD_3 (ρ_w = 0.85, p-value < 1e-04; $|\Delta AUC|_w$ = 0.031, p-value = 0.75) was the only gene set for whom results from Singscore could act as a proxy to its original models, except for study GSE34608 (Figure S4E).

482 ***Gene signatures after splitting***

483 Figure S5A-E shows the performance of 13 signatures as evaluated with their up/down
484 regulated subset of genes using ssGSEA, GSVA, and Singscore bidirectional scoring.
485 Notably, for the upregulated subset of Verhagen_10 , none of the datasets had AUCs
486 greater than 0.8, as given by ssGSEA and GSVA (Figure S5A-D). Study GSE101705
487 was the only selected study when evaluating the downregulated subset of Verhagen_10
488 using ssGSEA (ρ = 0.60, $|\Delta AUC|$ = 0.20), GSVA (ρ = 0.57, $|\Delta AUC|$ = 0.17), and
489 Singscore bidirectional scoring (ρ = -0.63, $|\Delta AUC|$ = 0.18; Figure S5B-E). However, it
490 showed different prediction results than the original models. Additionally, GSE107994
491 was selected for the downregulated subset of Verhagen_10 given by GSVA (ρ = 0.44,
492 $|\Delta AUC|$ = 0.19; Figure S5D).

493

494 ***ssGSEA with signature split vs. Original Model***

495 When assessing gene signatures based on their upregulated subset, all selected
496 studies had positive Spearman's rank correlations of the predicted scores given by
497 ssGSEA and original models (Figure S5A). More studies with high AUCs were selected
498 for 10 out of 12 gene signatures (excluding Leong_RISK_29 and Maertzdorf_15) when
499 evaluated with their respective upregulated genes using ssGSEA. Results from subsets
500 of Kaforou_27 and Kaforou_OD_53 showed similar diagnostic features when compared
501 to their original models, with highly correlated prediction scores (ρ_w > 0.80 for both gene
502 sets; p-value <= 1e-04) and small AUC differences ($|\Delta AUC|_w$ < 0.030 for both gene
503 sets; p-value > 0.080), and a study overlap coefficient of 1.00 for both gene sets (Figure
504 S5A).

505

506 When gene signatures were evaluated using their downregulated subsets, only
507 Maertzdorf_15 had an absolute Spearman's rank correlation greater than 0.80 (ρ_w: -
508 0.89, p-value <= 1e-05) and a small AUC difference ($|\Delta AUC|_w$ = 0.033, p-value = 0.010)
509 for results given by ssGSEA and its original model, with a study overlap coefficient of
510 1.00 (Figure S5B). Only Berry_393 (ρ_w = -0.62), Leong_24 (ρ_w = -0.64), and
511 Verhagen_10 (ρ_w = 0.60) had a more studies with high AUCs using ssGSEA (0.052 <
512 $|\Delta AUC|_w$ < 0.191; Figure S5B).

513

514 ***GSVA with signature split vs. Original Model***

515 Figure S5C shows that the predicted scores given by GSVA and original models are
516 positively correlated for most of the selected studies except GSE34608, for which the
517 study was negatively correlated when evaluated by the upregulated subsets of
518 Leong_24 (ρ = -0.11, $|\Delta AUC|$ = 0.25). Moreover, Kaforou_27 had the highest weighted
519 Spearman's rank correlation (ρ_w = 0.90, p-value < 1e-05) and the smallest AUC
520 difference ($|\Delta AUC|_w$ = 0.020, p-value = 0.68) among 12 gene sets when its upregulated
521 subset was assessed by GSVA, which presented an equivalent prediction pattern
522 compared to its original model (Figure S5C). The upregulated subset of Maertzdorf_15
523 was the only gene set whose original model results outperformed GSVA, which had a
524 greater number of studies with high AUCs from its original method (ρ_w = 0.68, $|\Delta AUC|_w$
525 = 0.094; Figure S5C).

526

527 When gene signatures were evaluated with their downregulated subsets, the results
528 from most of the gene sets given by GSVA underperformed the results from their
529 original models. Specifically, nine of 13 gene sets had a greater number of studies with
530 high AUCs based on the results from their original model (Figure S5D). Notably, no
531 datasets with high AUCs were selected when the downregulated subset of
532 Bloom_OD_144 and Kaforou_OD_44 were assessed by GSVA. GSE28623 was the
533 only study with high AUCs for the down-regulated subset of Anderson_42 (Figure S5D).
534 Maertzdorf_15's GSVA results, similar to those for the ssGSEA method, had the highest
535 absolute weighted Spearman's rank correlation (ρ_w = -0.88, p-value <= 1e-05) and the
536 smallest absolute AUC difference ($|\Delta AUC|_w$ = 0.03, p-value = 0.20) when compared to
537 its original model, with a study overlap coefficient of 1.00 (Figure S5D).

538

539

540 ***Singscore bidirectional scoring vs. Original Models***

541 Most of the selected studies had positive correlations for the predicted scores given by
542 Singscore bidirectional scoring and their original methods, except study GSE62525 from
543 Bloom_OD_144 and GSE101705 from Verhagen_10 (Figure S5E). Both Kaforou_27

544 and Kaforou_OD_53 had a weighted Spearman's rank correlation greater than 0.85 (p-
545 value < 1e-05 for both gene sets), absolute AUC difference smaller than 0.020 (p-
546 value > 0.05 for both gene sets), and study overlap coefficient of 1.00, which suggests
547 that results for these gene signatures given by Singscore bidirectional scoring could act
548 as a proxy from the results given by signatures' original models (Figure S5E).
549 Signatures Anderson_OD_51, Kaforou_OD_44, Maertzdorf_15, and Sambarey_HIV_10
550 had a larger number of studies with high AUCs given by their original model, weighted
551 Spearman's rank correlations between 0.53 and 0.86, and absolute AUC differences
552 ranging from 0.021 to 0.16 (Figure S5E).

553 **DISCUSSION**

554 TB diagnostics is moving toward using blood-based biomarkers, but serious gaps
555 remain in the analyses of these data. Here we evaluated the performance of 19 TB
556 gene signatures in distinguishing active TB from other clinical conditions using the
557 original published model and five different gene set scoring methods based on 24
558 transcriptomic studies. These datasets represent real-world heterogeneity concerning
559 geographic regions, host and pathogen genetics, and clinical context (34, 35, 37). Our
560 results suggested that an original gene signature model's predictive ability can be
561 improved or recaptured using gene set scoring methods.
562
563 The five gene set scoring methods used here belong to a class of methods that
564 compute a gene set enrichment score for each sample using only the genes from a
565 signature. However, some differences between methods are present. Gene set scoring
566 methods, including ssGSEA, GSVA, Zscore, and Singscore are *single-sample* methods
567 that rank genes in each sample individually by comparing the ranks of the signature
568 genes with the ranks of non-signature genes in the sample. By design, using these
569 single-sample methods, the score for an individual sample is not affected by other
570 samples in the cohort. In contrast, in computing an individual sample score, PLAGE
571 implements singular value decomposition (SVD) on the standardized gene expression
572 profile of all subjects in the dataset (50, 51, 53) such that sample composition had a
573 large effect on the PLAGE scores. In addition, the original models for the gene
574 signatures Sweeney_OD_3, Kaforou (Kaforou_27, Kafotrou_OD_44, and
575 Kaforou_OD_53), and Anderson (Anderson_42 and Anderson_OD_51) could also be
576 characterized as single sample methods, which rely on the expression of upregulated
577 and downregulated subset of genes within gene sets (Table 1). These single-sample
578 methods were more likely to produce robust scores for individual subjects, especially in
579 studies with small sample sizes or heterogeneous disease subtypes. Multi-sample
580 methods were susceptible to sample composition (i.e., the number of samples for
581 different subtypes), which could introduce biases if the size of samples for different
582 disease subtypes changed (53). PLAGE and other multi-sample biomarker models
583 (e.g., random forest, linear discriminant analysis, and K-nearest neighbors) compute a

584 different score for an individual sample whenever a patient enters or leaves the test
585 population. This is known as “test set bias” (62), as a gene signature’s performance
586 may be irreproducible when a patient population composition or size changes.
587 Therefore, one of the limitations of using these multi-sample methods for sample
588 scoring is that bias will be induced if researchers perform integration analysis by
589 merging datasets from different sources. In our study, the results given by PLAGE for
590 most of the signatures outperformed the rest of gene set scoring methods (Table 3;
591 Figure 2A). This is primarily because the gene signature selection process is usually
592 heavily based on prior knowledge and the activity levels of the selected genes are
593 biologically meaningful, which could be revealed using SVD-like methods, including
594 principal component analysis (51).
595
596 The weighted mean AUCs given by single-sample scoring methods were sometimes
597 lower than the AUC from the original model for some signatures (Table 3). For these
598 cases, the biomarker splitting strategy improved diagnostic ability when using the
599 single-sample scoring methods, ssGSEA, GSVA, and Singscore, consistent with
600 existing publications in other fields (50, 63). Further, we noted that the improvement of
601 weighted mean AUC values based on upregulated subsets was more dominant when
602 compared to the results from the downregulated subset (Table 3). This is likely because
603 upregulated genes are usually immune-related, such as FCGR1A/B, GBP5/6, C1QB,
604 SEPTIN4, and ANDKRD22 (21), which generate a clear signal in active TB and are
605 features of the immune response to the disease (64). The weighted AUCs from
606 Zak_RISK_16 were consistently greater than 0.80 for five gene set scoring methods
607 (Table 2), mainly due to the overexpression of all genes within Zak_RISK_16 relative to
608 its discovery dataset, with large number of genes being highly differentially expressed
609 from the recent Leicester clinical phenotype groups (64). Therefore, the choice of gene
610 set scoring method depends on the cohort composition and the differential expressed
611 genes within the gene signatures. Generally, it is ideal and efficient to implement gene
612 set scoring methods to evaluate the diagnostic accuracy of TB signatures, which we
613 have shown to achieve equivalent accuracy when compared to their original models.
614

The data preprocessing and training procedures are specialized and intractable for most TB gene signature discovery cases, which contributes to low generalizability in some biomarkers when evaluating their performance on independent datasets by implementing the original classification model. Both Berry_393 and Berry_OD_86 gene signatures used the K-nearest neighbor (KNN) algorithm, which demonstrated high classification ability in their discovery studies (Table 2) but had poor results across multiple studies (Figure 1). KNN clustering worked well when gene expression values were normalized to the median of each control group (65); however, performing such normalization for transcriptomic datasets originating from different clinical conditions or different platforms is unrealistic. KNN classification also assumes that similar inputs share similar labels; however, data points tend to be close together in high dimensional spaces (66). Since the Berry_393 and Berry_OD_86 consist of 393 and 86 transcripts respectively, KNN lost predictive power in transcriptomic studies containing few samples but large numbers of gene expression features.

On the other hand, the performance of Verhagen_10 was poor across independent studies based on the results given by its original diagnostic model but had AUC values equal to 1.00 in datasets GSE81746 and GSE41055 (Figure 1). GSE41055 is the discovery study for Verhagen_10, and GSE81746 is a small study that only contains two active TB diseases and four health control samples. In our comparison, 17 of 19 signatures could identify the active TB subtype with an AUC greater than 0.80 (Figure 1). The mediocre performance of Verhagen_10 across multiple studies is a sign of overfitting, a common problem using random forest, which relies on optimizing the tuning parameters (26). Since the original publication did not offer information about the hyper-parameters, we could not reconstruct the diagnostic model in the same way. Similar observations were made for Leong_RISK_29 (19), for which AUC results varied from 0.5 and 1.00 across independent datasets (Figure 1). As Leong_RISK_29 was designed to capture early host response to infection, it has not been generalized to samples with clinical manifestations of the disease (32). In these and many other ways, a gene signature's diagnostic accuracy may be underestimated by evaluating its performance using its original model.

646 We also examined the gene signatures' predictive accuracy within individual studies
647 based on the results given by gene set scoring methods and the signatures' original
648 model. Results from PLAGE and ssGSEA for Kaforou_27 were highly correlated (ρ_w
649 from PLAGE: = -0.92, ρ_w from ssGSEA: = 0.78), with a small AUC difference ($|\Delta AUC|_w$
650 from PLAGE: = 0.030, $|\Delta AUC|_w$ from ssGSEA: = 0.032), and it had a study overlap
651 coefficient of 1.00 when compared to its original model (Figure S4A-B). This is primarily
652 because of the presence of 21 overexpressed genes within the Kaforou_27 gene set,
653 which dominates the performance of the gene signatures (Figure S5A). We identified a
654 similar situation for Maertzdorf_15, which had 12 downregulated genes within its gene
655 set. Maertzdorf_15 and its downregulated subsets had consistently high negative
656 Spearman's rank correlations (-0.89 <= ρ_w <= -0.78) for the prediction scores given by
657 its original model and gene set scoring methods except for PLAGE (ρ_w = 0.94) and
658 Singscore bidirectional scoring (ρ_w = 0.86; Figure S4 A-E; Figure S5B, D-E). The
659 outperformance of Sweeney_OD_3 in ssGSEA and Singscore unidirectional scoring
660 was largely due to the down-regulated gene *KLF2* within the Sweeney_OD_3 gene set.
661 It has a relatively lower summary effect of the standardized mean difference between
662 active tuberculosis and other clinical conditions from the biomarker's original discovery
663 datasets of Sweeney_OD_3; in contrast, the remaining two upregulated genes were
664 highly differentially expressed in the corresponding datasets (26).
665
666 Our study has several limitations. We only compared the performance of active TB
667 disease versus all other disease states regardless of how TB was diagnosed, and we
668 did not perform subgroup analysis stratified by different clinical conditions, such as age,
669 region, gender, or comorbidities. Additionally, some reconstructed signature models
670 may not be the same as those used in the original publication, as some of these
671 publications do not provide precise details to recreate the original training model.
672 Instead, we followed the details outlined in the previously published comparison of
673 Warsinske *et al.* (19). Due to different naming sequencing platforms for transcripts,
674 some genes within signatures were missing across multiple studies, and we could not
675 evaluate the biomarkers' diagnostic ability in those cases accurately. Although we used
676 KNN imputation to estimate the expression values for those missing genes in the

validation study, the imputation process may have potentially led to bias. Our comparison would still be valid if we followed similar procedures to handle missing values across independent studies.

In conclusion, we showed that gene set scoring methods are effective for evaluating gene signature accuracy for comparing active TB disease versus other clinical conditions. These methods perform similarly when compared to the signatures' original models. Overall, the performance of TB biomarkers across multiple studies was similar between the PLAGE and the original models. The methods ssGSEA, GSVA, and Singscore can also capture the diagnostic accuracy of gene signatures by taking the gene directional information within gene sets into account. Given the challenges associated with rebuilding or re-evaluating the signatures' original biomarker model(s), gene set scoring methods could serve as a reliable alternative computational methodology to apply or perform comparisons of TB biomarkers.

691 **REFERNCES**

692 1. World Health Organization. *Global Tuberculosis Report 2020*. World Health
693 Organization; 2020.
694 2. Pai M, Behr MA, Dowdy D, Dheda K, Divangahi M, Boehme CC, Ginsberg A,
695 Swaminathan S, Spigelman M, Getahun H, Menzies D, Raviglione M. Tuberculosis.
696 *Nat Rev Dis Primers* 2016;2:16076.
697 3. Park JH, Choe J, Bae M, Choi S, Jung KH, Kim MJ, Chong YP, Lee S-O, Choi S-H,
698 Kim YS, Woo JH, Jo K-W, Shim TS, Kim MY, Kim S-H. Clinical Characteristics and
699 Radiologic Features of Immunocompromised Patients With Pauci-Bacillary
700 Pulmonary Tuberculosis Receiving Delayed Diagnosis and Treatment. *Open Forum*
701 *Infect Dis* 2019;6:ofz002.
702 4. Swaminathan S, Ramachandran G. Challenges in childhood tuberculosis. *Clin*
703 *Pharmacol Ther* 2015;98:240–244.
704 5. Sharma SK, Ryan H, Khaparde S, Sachdeva KS, Singh AD, Mohan A, Sarin R,
705 Paramasivan CN, Kumar P, Nischal N, Khatiwada S, Garner P, Tharyan P. Index-
706 TB guidelines: Guidelines on extrapulmonary tuberculosis for India. *Indian J Med*
707 *Res* 2017;145:448–463.
708 6. Gaur M, Singh A, Sharma V, Tandon G, Bothra A, Vasudeva A, Kedia S, Khanna
709 A, Khanna V, Lohiya S, Varma-Basil M, Chaudhry A, Misra R, Singh Y. Diagnostic
710 performance of non-invasive, stool-based molecular assays in patients with
711 paucibacillary tuberculosis. *Sci Rep* 2020;10:7102.
712 7. Gupta RK, Turner CT, Venturini C, Esmail H, Rangaka MX, Copas A, Lipman M,
713 Abubakar I, Noursadeghi M. Concise whole blood transcriptional signatures for
714 incipient tuberculosis: a systematic review and patient-level pooled meta-analysis.

715 *Lancet Respir Med* 2020;8:395–406.

716 8. Sloot R, Schim van der Loeff MF, van Zwet EW, Haks MC, Keizer ST, Scholing M,
717 Ottenhoff THM, Borgdorff MW, Joosten SA. Biomarkers Can Identify Pulmonary
718 Tuberculosis in HIV-infected Drug Users Months Prior to Clinical Diagnosis.
719 *EBioMedicine* 2015;2:172–179.

720 9. Esmail H, Lai RP, Lesosky M, Wilkinson KA, Graham CM, Horswell S, Coussens
721 AK, Barry CE 3rd, O'Garra A, Wilkinson RJ. Complement pathway gene activation
722 and rising circulating immune complexes characterize early disease in HIV-
723 associated tuberculosis. *Proc Natl Acad Sci U S A* 2018;115:E964–E973.

724 10. Berry MPR, Graham CM, McNab FW, Xu Z, Bloch SAA, Oni T, Wilkinson KA,
725 Banchereau R, Skinner J, Wilkinson RJ, Quinn C, Blankenship D, Dhawan R, Cush
726 JJ, Mejias A, Ramilo O, Kon OM, Pascual V, Banchereau J, Chaussabel D,
727 O'Garra A. An interferon-inducible neutrophil-driven blood transcriptional signature
728 in human tuberculosis. *Nature* 2010;466:973–977.

729 11. Walter ND, Miller MA, Vasquez J, Weiner M, Chapman A, Engle M, Higgins M,
730 Quinones AM, Rosselli V, Canono E, Yoon C, Cattamanchi A, Davis JL, Phang T,
731 Stearman RS, Datta G, Garcia BJ, Daley CL, Strong M, Kechris K, Fingerlin TE,
732 Reves R, Geraci MW. Blood Transcriptional Biomarkers for Active Tuberculosis
733 among Patients in the United States: a Case-Control Study with Systematic Cross-
734 Classifier Evaluation. *J Clin Microbiol* 2016;54:274–282.

735 12. Kaforou M, Wright VJ, Oni T, French N, Anderson ST, Bangani N, Banwell CM,
736 Brent AJ, Crampin AC, Dockrell HM, Eley B, Heyderman RS, Hibberd ML, Kern F,
737 Langford PR, Ling L, Mendelson M, Ottenhoff TH, Zgambo F, Wilkinson RJ, Coin

738 LJ, Levin M. Detection of tuberculosis in HIV-infected and -uninfected African adults
739 using whole blood RNA expression signatures: a case-control study. *PLoS Med*
740 2013;10:e1001538.
741 13. Suliman S, Thompson EG, Sutherland J, Weiner J 3rd, Ota MOC, Shankar S,
742 Penn-Nicholson A, Thiel B, Erasmus M, Maertzdorf J, Duffy FJ, Hill PC, Hughes
743 EJ, Stanley K, Downing K, Fisher ML, Valvo J, Parida SK, van der Spuy G, Tromp
744 G, Adetifa IMO, Donkor S, Howe R, Mayanja-Kizza H, Boom WH, Dockrell HM,
745 Ottenhoff THM, Hatherill M, Aderem A, *et al.* Four-Gene Pan-African Blood
746 Signature Predicts Progression to Tuberculosis. *Am J Respir Crit Care Med*
747 2018;197:1198–1208.
748 14. Zak DE, Penn-Nicholson A, Scriba TJ, Thompson E, Suliman S, Amon LM,
749 Mahomed H, Erasmus M, Whatney W, Hussey GD, Abrahams D, Kafaar F,
750 Hawkridge T, Verver S, Hughes EJ, Ota M, Sutherland J, Howe R, Dockrell HM,
751 Boom WH, Thiel B, Ottenhoff THM, Mayanja-Kizza H, Crampin AC, Downing K,
752 Hatherill M, Valvo J, Shankar S, Parida SK, *et al.* A blood RNA signature for
753 tuberculosis disease risk: a prospective cohort study. *Lancet* 2016;387:2312–2322.
754 15. Thompson EG, Du Y, Malherbe ST, Shankar S, Braun J, Valvo J, Ronacher K,
755 Tromp G, Tabb DL, Alland D, Shenai S, Via LE, Warwick J, Aderem A, Scriba TJ,
756 Winter J, Walzl G, Zak DE, Catalysis TB–Biomarker Consortium. Host blood RNA
757 signatures predict the outcome of tuberculosis treatment. *Tuberculosis*
758 2017;107:48–58.
759 16. Singhania A, Verma R, Graham CM, Lee J, Tran T, Richardson M, Lecine P,
760 Leissner P, Berry MPR, Wilkinson RJ, Kaiser K, Rodrigue M, Woltmann G, Haldar

761 P, O'Garra A. A modular transcriptional signature identifies phenotypic
762 heterogeneity of human tuberculosis infection. *Nat Commun* 2018;9:2308.
763 17. Roe J, Venturini C, Gupta RK, Gurry C, Chain BM, Sun Y, Southern J, Jackson C,
764 Lipman MC, Miller RF, Martineau AR, Abubakar I, Noursadeghi M. Blood
765 Transcriptomic Stratification of Short-term Risk in Contacts of Tuberculosis. *Clin*
766 *Infect Dis* 2020;70:731–737.
767 18. Scriba TJ, Fiore-Gartland A, Penn-Nicholson A, Mulenga H, Kimbung Mbandi S,
768 Borate B, Mendelsohn SC, Hadley K, Hikuam C, Kaskar M, Musvosvi M, Bilek N,
769 Self S, Sumner T, White RG, Erasmus M, Jaxa L, Raphela R, Innes C, Brumskine
770 W, Hiemstra A, Malherbe ST, Hassan-Moosa R, Tameris M, Walzl G, Naidoo K,
771 Churchyard G, Hatherill M, CORTIS-01 Study Team. Biomarker-guided
772 tuberculosis preventive therapy (CORTIS): a randomised controlled trial. *Lancet*
773 *Infect Dis* 2021;21:354–365.
774 19. Warsinske H, Vashisht R, Khatri P. Host-response-based gene signatures for
775 tuberculosis diagnosis: A systematic comparison of 16 signatures. *PLoS Med*
776 2019;16:e1002786.
777 20. Noble WS. What is a support vector machine? *Nat Biotechnol* 2006;24:1565–1567.
778 21. Johnson WE, Odom A, Cintron C, Muthaiah M, Knudsen S, Joseph N, Babu S,
779 Lakshminarayanan S, Jenkins DF, Zhao Y, Nankya E, Horsburgh CR, Roy G,
780 Ellner JJ, Sarkar S, Salgame P, Hochberg NS. Comparing Tuberculosis Gene
781 Signatures in Malnourished Individuals using the TBSignatureProfiler. *BMC Infect*
782 *Dis* 2020;
783 22. Laux da Costa L, Delcroix M, Dalla Costa ER, Prestes IV, Milano M, Francis SS,

784 Unis G, Silva DR, Riley LW, Rossetti MLR. A real-time PCR signature to
785 discriminate between tuberculosis and other pulmonary diseases. *Tuberculosis*
786 2015;95:421–425.
787 23. Jacobsen M, Repsilber D, Gutschmidt A, Neher A, Feldmann K, Mollenkopf HJ,
788 Ziegler A, Kaufmann SHE. Candidate biomarkers for discrimination between
789 infection and disease caused by Mycobacterium tuberculosis. *J Mol Med*
790 2007;85:613–621.
791 24. Sambarey A, Devaprasad A, Mohan A, Ahmed A, Nayak S, Swaminathan S,
792 D'Souza G, Jesuraj A, Dhar C, Babu S, Vyakarnam A, Chandra N. Unbiased
793 Identification of Blood-based Biomarkers for Pulmonary Tuberculosis by Modeling
794 and Mining Molecular Interaction Networks. *EBioMedicine* 2017;15:112–126.
795 25. Hänzelmann S, Castelo R, Guinney J. GSVA: gene set variation analysis for
796 microarray and RNA-seq data. *BMC Bioinformatics* 2013;14:7.
797 26. Sweeney TE, Braviak L, Tato CM, Khatri P. Genome-wide expression for diagnosis
798 of pulmonary tuberculosis: a multicohort analysis. *Lancet Respir Med* 2016;4:213–
799 224.
800 27. Anderson ST, Kaforou M, Brent AJ, Wright VJ, Banwell CM, Chagaluka G, Crampin
801 AC, Dockrell HM, French N, Hamilton MS, Hibberd ML, Kern F, Langford PR, Ling
802 L, Mlotha R, Ottenhoff THM, Pienaar S, Pillay V, Scott JAG, Twahir H, Wilkinson
803 RJ, Coin LJ, Heyderman RS, Levin M, Eley B. Diagnosis of childhood tuberculosis
804 and host RNA expression in Africa. *N Engl J Med* 2014;370:1712–1723.
805 28. Bloom CI, Graham CM, Berry MPR, Rozakeas F, Redford PS, Wang Y, Xu Z,
806 Wilkinson KA, Wilkinson RJ, Kendrick Y, Devouassoux G, Ferry T, Miyara M,

807 Bouvry D, Valeyre D, Gorochov G, Blankenship D, Saadatian M, Vanhems P,
808 Beynon H, Vancheeswaran R, Wickremasinghe M, Chaussabel D, Banchereau J,
809 Pascual V, Ho L-P, Lipman M, O'Garra A. Transcriptional blood signatures
810 distinguish pulmonary tuberculosis, pulmonary sarcoidosis, pneumonias and lung
811 cancers. *PLoS One* 2013;8:e70630.
812 29. Leong S, Zhao Y, Joseph NM, Hochberg NS, Sarkar S, Pleskunas J, Hom D,
813 Lakshminarayanan S, Horsburgh CR Jr, Roy G, Ellner JJ, Johnson WE, Salgame
814 P. Existing blood transcriptional classifiers accurately discriminate active
815 tuberculosis from latent infection in individuals from south India. *Tuberculosis*
816 2018;109:41–51.
817 30. Maertzdorf J, McEwen G, Weiner J 3rd, Tian S, Lader E, Schriek U, Mayanja-Kizza
818 H, Ota M, Kenneth J, Kaufmann SH. Concise gene signature for point-of-care
819 classification of tuberculosis. *EMBO Mol Med* 2016;8:86–95.
820 31. Verhagen LM, Zomer A, Maes M, Villalba JA, Del Nogal B, Eleveld M, van Hijum
821 SA, de Waard JH, Hermans PW. A predictive signature gene set for discriminating
822 active from latent tuberculosis in Warao Amerindian children. *BMC Genomics*
823 2013;14:74.
824 32. Leong S, Zhao Y, Ribeiro-Rodrigues R, Jones-López EC, Acuña-Villaorduña C,
825 Rodrigues PM, Palaci M, Alland D, Dietze R, Ellner JJ, Johnson WE. Cross-
826 validation of existing signatures and derivation of a novel 29-gene transcriptomic
827 signature predictive of progression to TB in a Brazilian cohort of household
828 contacts of pulmonary TB. *Tuberculosis* 2020;120:101898.
829 33. Banchereau R, Jordan-Villegas A, Ardura M, Mejias A, Baldwin N, Xu H, Saye E,

830 Rossello-Urgell J, Nguyen P, Blankenship D, Creech CB, Pascual V, Banchereau
831 J, Chaussabel D, Ramilo O. Host immune transcriptional profiles reflect the
832 variability in clinical disease manifestations in patients with Staphylococcus aureus
833 infections. *PLoS One* 2012;7:e34390.
834 34. Park J, Munagala I, Xu H, Blankenship D, Maffucci P, Chaussabel D, Banchereau
835 J, Pascual V, Cunningham-Rundles C. Interferon signature in the blood in
836 inflammatory common variable immune deficiency. *PLoS One* 2013;8:e74893.
837 35. Obermoser G, Presnell S, Domico K, Xu H, Wang Y, Anguiano E, Thompson-
838 Snipes L, Ranganathan R, Zeitner B, Bjork A, Anderson D, Speake C, Ruchaud E,
839 Skinner J, Alsina L, Sharma M, Dutartre H, Cepika A, Israelsson E, Nguyen P,
840 Nguyen Q-A, Harrod AC, Zurawski SM, Pascual V, Ueno H, Nepom GT, Quinn C,
841 Blankenship D, Palucka K, *et al.* Systems scale interactive exploration reveals
842 quantitative and qualitative differences in response to influenza and pneumococcal
843 vaccines. *Immunity* 2013;38:831–844.
844 36. VanValkenburg A, Kaipilyawar V, Sarkar S, Lakshminarayanan S, Cintron C,
845 Prakash Babu S, Knudsen S, Joseph NM, Horsburgh CR, Ellner JJ, Narasimhan
846 PB, Johnson WE, Hochberg NS, Salgame P. Malnutrition leads to increased
847 inflammation and expression of tuberculosis risk signatures in recently exposed
848 household contacts of pulmonary tuberculosis. *Front Immunol* 2022;13:1011166.
849 37. Maertzdorf J, Ota M, Repsilber D, Mollenkopf HJ, Weiner J, Hill PC, Kaufmann
850 SHE. Functional correlations of pathogenesis-driven gene expression signatures in
851 tuberculosis. *PLoS One* 2011;6:e26938.
852 38. Elliott TOJP, Owolabi O, Donkor S, Kampmann B, Hill PC, Ottenhoff THM, Haks

853 MC, Kaufmann SHE, Maertzdorf J, Sutherland JS. Dysregulation of apoptosis is a
854 risk factor for tuberculosis disease progression. *J Infect Dis* 2015;212:1469–1479.
855 39. Blankley S, Graham CM, Turner J, Berry MPR, Bloom CI, Xu Z, Pascual V,
856 Banchereau J, Chaussabel D, Breen R, Santis G, Blankenship DM, Lipman M,
857 O'Garra A. The transcriptional signature of active tuberculosis reflects symptom
858 status in extra-pulmonary and pulmonary tuberculosis. *PLoS One*
859 2016;11:e0162220.
860 40. Cai Y, Yang Q, Tang Y, Zhang M, Liu H, Zhang G, Deng Q, Huang J, Gao Z, Zhou
861 B, Feng CG, Chen X. Increased complement C1q level marks active disease in
862 human tuberculosis. *PLoS One* 2014;9:e92340.
863 41. Maertzdorf J, Weiner J 3rd, Mollenkopf H-J, TBornotTB Network, Bauer T, Prasse
864 A, Müller-Quernheim J, Kaufmann SHE. Common patterns and disease-related
865 signatures in tuberculosis and sarcoidosis. *Proc Natl Acad Sci U S A*
866 2012;109:7853–7858.
867 42. Ottenhoff THM, Dass RH, Yang N, Zhang MM, Wong HEE, Sahiratmadja E, Khor
868 CC, Alisjahbana B, van Crevel R, Marzuki S, Seielstad M, van de Vosse E, Hibberd
869 ML. Genome-wide expression profiling identifies type 1 interferon response
870 pathways in active tuberculosis. *PLoS One* 2012;7:e45839.
871 43. Dawany N, Showe LC, Kossenkov AV, Chang C, Ive P, Conradie F, Stevens W,
872 Sanne I, Azzoni L, Montaner LJ. Identification of a 251 gene expression signature
873 that can accurately detect M. tuberculosis in patients with and without HIV co-
874 infection. *PLoS One* 2014;9:e89925.
875 44. Marais S, Lai RPJ, Wilkinson KA, Meintjes G, O'Garra A, Wilkinson RJ.

876 Inflammasome activation underlying central nervous system deterioration in HIV-
877 associated tuberculosis. *J Infect Dis* 2017;215:677–686.
878 45. de Araujo LS, Vaas LAI, Ribeiro-Alves M, Geffers R, Mello FCQ, de Almeida AS,
879 Moreira A da SR, Kritski AL, Lapa E Silva JR, Moraes MO, Pessler F, Saad MHF.
880 Transcriptomic biomarkers for tuberculosis: Evaluation of DOCK9. EPHA4, and
881 NPC2 mRNA expression in peripheral blood. *Front Microbiol* 2016;7:1586.
882 46. Zak DE, Penn-Nicholson A, Scriba TJ, Thompson E, Suliman S, Amon LM,
883 Mahomed H, Erasmus M, Whatney W, Hussey GD, Abrahams D, Kafaar F,
884 Hawkridge T, Verver S, Hughes EJ, Ota M, Sutherland J, Howe R, Dockrell HM,
885 Boom WH, Thiel B, Ottenhoff THM, Mayanja-Kizza H, Crampin AC, Downing K,
886 Hatherill M, Valvo J, Shankar S, Parida SK, *et al.* A blood RNA signature for
887 tuberculosis disease risk: a prospective cohort study. *Lancet* 2016;387:2312–2322.
888 47. Lee S-W, Wu LS-H, Huang G-M, Huang K-Y, Lee T-Y, Weng JT-Y. Gene
889 expression profiling identifies candidate biomarkers for active and latent
890 tuberculosis. *BMC Bioinformatics* 2016;17 Suppl 1:3.
891 48. Tientcheu LD, Maertzdorf J, Weiner J, Adetifa IM, Mollenkopf H-J, Sutherland JS,
892 Donkor S, Kampmann B, Kaufmann SHE, Dockrell HM, Ota MO. Differential
893 transcriptomic and metabolic profiles of M. africanum- and M. tuberculosis-infected
894 patients after, but not before, drug treatment. *Genes Immun* 2015;16:347–355.
895 49. Pavlov YL. *Random Forests*. Walter de Gruyter GmbH & Co KG; 2019.
896 50. Subramanian A, Tamayo P, Mootha VK, Mukherjee S, Ebert BL, Gillette MA,
897 Paulovich A, Pomeroy SL, Golub TR, Lander ES, Mesirov JP. Gene set enrichment
898 analysis: a knowledge-based approach for interpreting genome-wide expression

899 profiles. *Proc Natl Acad Sci U S A* 2005;102:15545–15550.

900 51. Tomfohr J, Lu J, Kepler TB. Pathway level analysis of gene expression using
901 singular value decomposition. *BMC Bioinformatics* 2005;6:225.

902 52. Lee E, Chuang H-Y, Kim J-W, Ideker T, Lee D. Inferring pathway activity toward
903 precise disease classification. *PLoS Comput Biol* 2008;4:e1000217.

904 53. Foroutan M, Bhuva DD, Lyu R, Horan K, Cursons J, Davis MJ. Single sample
905 scoring of molecular phenotypes. *BMC Bioinformatics* 2018;19:404.

906 54. Love MI, Huber W, Anders S. Moderated estimation of fold change and dispersion
907 for RNA-seq data with DESeq2. *Genome Biol* 2014;15:550.

908 55. Ritchie ME, Phipson B, Wu D, Hu Y, Law CW, Shi W, Smyth GK. limma powers
909 differential expression analyses for RNA-sequencing and microarray studies.
910 *Nucleic Acids Res* 2015;43:e47–e47.

911 56. Oh S, Abdelnabi J, Al-Dulaimi R, Aggarwal A, Ramos M, Davis S, Riester M,
912 Waldron L. HGNChelper: identification and correction of invalid gene symbols for
913 human and mouse. *F1000Res* 2020;9:1493.

914 57. Hastie T, Tibshirani R, Narasimhan B, Chu G. *impute: Imputation for microarray*
915 *data*. 2020. at <10.18129/B9.bioc.impute>.

916 58. Zhang Y, Jenkins DF, Manimaran S, Johnson WE. Alternative empirical Bayes
917 models for adjusting for batch effects in genomic studies. *BMC Bioinformatics*
918 2018;19:262.

919 59. Johnson WE, Li C, Rabinovic A. Adjusting batch effects in microarray expression
920 data using empirical Bayes methods. *Biostatistics* 2007;8:118–127.

921 60. Khan MRA, Brandenburger T. *ROCit: Performance Assessment of Binary Classifier*

922 *with Visualization*. 2020. at <https://CRAN.R-project.org/package=ROCit>.

923 61. M.k V, K K. A survey on similarity measures in text mining. *Mach Learn Appl Int J*
924 2016;3:19–28.

925 62. Patil P, Bachant-Winner P-O, Haibe-Kains B, Leek JT. Test set bias affects
926 reproducibility of gene signatures. *Bioinformatics* 2015;31:2318–2323.

927 63. Barbie DA, Tamayo P, Boehm JS, Kim SY, Moody SE, Dunn IF, Schinzel AC,
928 Sandy P, Meylan E, Scholl C, Fröhling S, Chan EM, Sos ML, Michel K, Mermel C,
929 Silver SJ, Weir BA, Reiling JH, Sheng Q, Gupta PB, Wadlow RC, Le H, Hoersch S,
930 Wittner BS, Ramaswamy S, Livingston DM, Sabatini DM, Meyerson M, Thomas
931 RK, *et al.* Systematic RNA interference reveals that oncogenic KRAS-driven
932 cancers require TBK1. *Nature* 2009;462:108–112.

933 64. Tabone O, Verma R, Singhania A, Chakravarty P, Branchett WJ, Graham CM, Lee
934 J, Trang T, Reynier F, Leissner P, Kaiser K, Rodrigue M, Woltmann G, Haldar P,
935 O'Garra A. Blood transcriptomics reveal the evolution and resolution of the immune
936 response in tuberculosis. *J Exp Med* 2021;218:.

937 65. Tran TN, Wehrens R, Buydens LMC. KNN-kernel density-based clustering for high-
938 dimensional multivariate data. *Computational Statistics & Data Analysis* 2006;

939 66. Lulli A, Oneto L, Anguita D. Mining big data with random forests. *Cognit Comput*
940 2019;11:294–316.

Table 1. Summary of TB gene signatures compared in this study and their original training model.

Signature Name	Gene Signature Number	Comparison	Datasets	Original Model Description
Sweeney_OD_3	3	Active tuberculosis vs. (LTBI & HCs & OD)	GSE19491 & GSE42834 & GSE37250	Difference of geometric means between up and downregulated genes
Jacobsen_3	3	Active tuberculosis vs. LTBI	GSE19491	Linear Discriminant Analysis
LauxdaCosta_OD_3	3	Active tuberculosis vs. OD	GSE42834	Random Forest
Maertzdorf_4	4	Active tuberculosis vs. HCs	GSE74092	Random Forest
Sambarey_HIV_10	10	Active tuberculosis vs. OD	GSE37250	Linear Discriminant Analysis
Verhagen_10	10	Active tuberculosis vs. (LTBI & HCs)	GSE41055	Random Forest
Maertzdorf_15	15	Active tuberculosis vs. HCs	GSE74092	Random Forest
Leong_24	24	Active tuberculosis vs. LTBI	GSE10175	Ridge Logistic Regression
Kaforou_27	27	Active tuberculosis vs. OD	GSE19491	Difference of arithmetic means between up and downregulated genes
Anderson_42	42	Active tuberculosis vs. LTBI	GSE39940	Difference of sums between up and downregulated genes
Kaforou_OD_44	44	Active tuberculosis vs. OD	GSE19491	Difference of arithmetic means between up and downregulated genes
Anderson_OD_51	51	Active tuberculosis vs. OD	GSE39940	Difference of sums between up and downregulated genes
Kaforou_OD_53	53	Active tuberculosis vs. OD	GSE19491	Difference of arithmetic means between up and downregulated genes
Berry_OD_86	86	Active tuberculosis vs. OD	GSE19491	K-nearest neighbors algorithm
Bloom_OD_144	144	Active tuberculosis vs. (HCs & OD)	GSE42834	Support Vector Machines
Berry_393	393	Active tuberculosis vs. (LTBI & HCs)	GSE19491	K-nearest neighbors algorithm
Suliman_RISK_4	4	Incipient tuberculosis vs. HCs	GSE94438	Support Vector Machines (linear kernel, using paired ratio)
Zak_RISK_16	16	Incipient tuberculosis vs. HCs	GSE79362	Support Vector Machines (linear kernel)
Leong_RISK_29	29	Incipient tuberculosis vs. HCs	GSE79362	Lasso Logistic Regression

Figure 1. Heatmap of AUC distribution for each signature across 24 studies using original model. Grids with black borders were the discovery sets for each TB gene signature. Each row represents one signature. Signatures were clustered into different categories with respect to the TB subtypes that they aim to identify. The column of the heatmap representing the studies that were used in this paper. The datasets were rearranged in decreasing order based on their mean AUC values across all TB gene signatures.

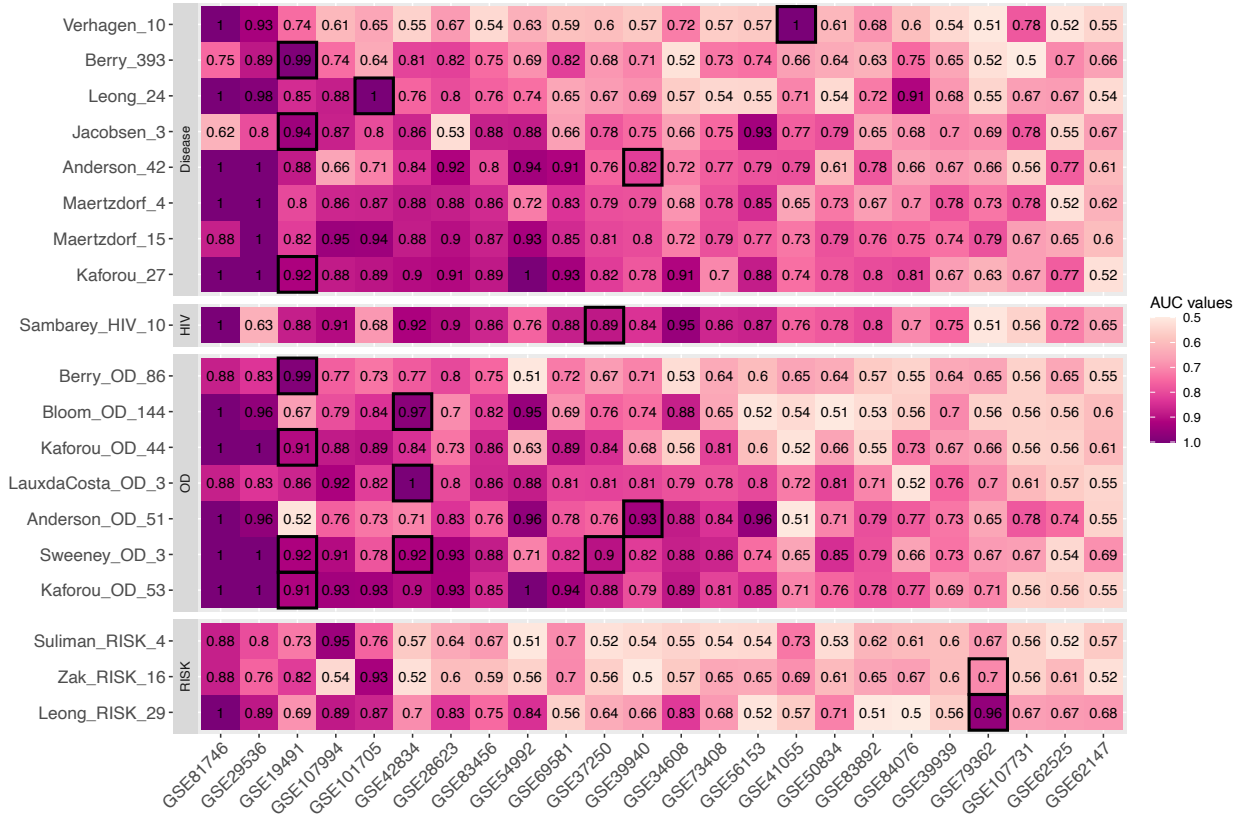

Table 2. Weighted mean AUC and 95% CI for 19 gene signatures using original model and gene set scoring methods (ssGSEA, GSVA, PLAGE, Zscore, and Singscore) across 24 studies. Color-coded for AUC values that were 0.05 unit greater (red) than in Warsinske et al and were 0.05 less (blue) than Warsinske et al. (*: p <= 0.01, **: p <= 0.001, ***: p <= 0.0001 derived from Wilcoxon signed-rank test between the original model and corresponding gene set scoring methods; †: the original model results underperformed the Warsinske et al. with more than 0.05 unit; ‡: the original model results outperformed the Warsiske et al. with more than 0.05 unit).

Signature	Warsinske et al.	TBSignatureProfiler (Original Model)	TBSignatureProfiler (ssGSEA)	TBSignatureProfiler (GSVA)	TBSignatureProfiler (PLAGE)	TBSignatureProfiler (Zscore)	TBSignatureProfiler (Singscore)
LauxdaCosta_OD_3	0.76 (0.45–1.00)	0.80 (0.76-0.83)	0.82 (0.76-0.86)	0.79 (0.74-0.83)	0.83* (0.79-0.86)	0.78 (0.74-0.80)	0.82 (0.75-0.86)
Jacobsen_3	0.83 (0.69–0.98)	0.76† (0.71-0.80)	0.72 (0.68-0.76)	0.69 (0.64-0.73)	0.78 (0.75-0.81)	0.69 (0.65-0.73)	0.71 (0.67-0.75)
Sweeney_OD_3	0.85 (0.72–0.99)	0.81 (0.76-0.85)	0.82 (0.77-0.86)	0.75 (0.69-0.80)	0.82 (0.78-0.85)	0.77 (0.71-0.82)	0.82 (0.77-0.86)
Maertzdorf_4	0.79 (0.64–0.95)	0.80 (0.77-0.83)	0.70* (0.65-0.75)	0.73** (0.69-0.78)	0.81 (0.78-0.85)	0.72** (0.68-0.76)	0.66* (0.62-0.72)
Verhagen_10	0.54 (0.41–0.68)	0.61‡ (0.57-0.66)	0.57 (0.55-0.60)	0.59 (0.56-0.64)	0.65 (0.59-0.71)	0.62 (0.57-0.68)	0.58 (0.55-0.61)
Sambarey_HIV_10	0.82 (0.57–1.00)	0.83 (0.76-0.87)	0.80 (0.76-0.84)	0.80 (0.76-0.84)	0.76 (0.70-0.83)	0.75 (0.70-0.81)	0.79 (0.75-0.83)
Maertzdorf_15	0.79 (0.66–0.92)	0.82 (0.79-0.85)	0.83 (0.79-0.87)	0.82 (0.78-0.86)	0.83 (0.80-0.86)	0.79 (0.75-0.82)	0.79 (0.75-0.84)
Leong_24	0.75 (0.54–0.95)	0.72 (0.67-0.78)	0.73 (0.70-0.77)	0.61 (0.58-0.65)	0.73 (0.67-0.79)	0.61 (0.58-0.65)	0.73 (0.69-0.78)
Kaforou_27	0.83 (0.64–1.00)	0.81 (0.77-0.85)	0.82 (0.78-0.85)	0.79 (0.76-0.82)	0.83 (0.79-0.87)	0.79 (0.76-0.82)	0.78 (0.73-0.82)
Anderson_42	0.82 (0.66–0.97)	0.78 (0.73-0.83)	0.61** (0.58-0.66)	0.60** (0.58-0.64)	0.76 (0.70-0.82)	0.65** (0.59-0.73)	0.57** (0.53-0.61)
Kaforou_OD_44	0.78 (0.56–1.00)	0.76 (0.69-0.81)	0.67 (0.63-0.71)	0.72 (0.68-0.74)	0.80 (0.72-0.86)	0.70 (0.67-0.74)	0.70 (0.67-0.74)
Anderson_OD_51	0.58 (0.33–0.82)	0.71‡ (0.64-0.78)	0.75 (0.71-0.80)	0.81 (0.77-0.84)	0.79 (0.72-0.85)	0.75 (0.66-0.82)	0.77 (0.73-0.80)
Kaforou_OD_53	0.84 (0.70–0.99)	0.83 (0.78-0.87)	0.70** (0.66-0.75)	0.77** (0.74-0.80)	0.84 (0.80-0.87)	0.77** (0.73-0.80)	0.77** (0.73-0.81)
Berry_OD_86	0.69 (0.36–1.00)	0.69 (0.66-0.72)	0.71 (0.68-0.76)	0.74 (0.70-0.78)	0.75* (0.72-0.80)	0.73 (0.69-0.78)	0.73 (0.68-0.78)
Bloom_OD_144	0.74 (0.52–0.96)	0.70 (0.66-0.74)	0.77 (0.72-0.81)	0.76 (0.71-0.81)	0.71 (0.66-0.78)	0.70 (0.63-0.77)	0.76 (0.71-0.81)
Berry_393	0.71 (0.43–0.99)	0.70 (0.66-0.74)	0.78 (0.74-0.82)	0.77 (0.73-0.81)	0.79* (0.75-0.84)	0.77 (0.73-0.81)	0.79 (0.74-0.84)
Suliman_RISK_4	NA	0.62 (0.57-0.69)	0.62 (0.58-0.68)	0.55 (0.53-0.58)	0.74** (0.70-0.79)	0.60 (0.55-0.66)	0.61 (0.56-0.66)
Zak_RISK_16	NA	0.62 (0.56-0.70)	0.85*** (0.81-0.88)	0.84*** (0.80-0.88)	0.83*** (0.80-0.86)	0.83*** (0.79-0.86)	0.84*** (0.80-0.88)
Leong_RISK_29	NA	0.68 (0.65-0.73)	0.58* (0.56-0.61)	0.59* (0.56-0.61)	0.75 (0.70-0.80)	0.60 (0.56-0.64)	0.61* (0.57-0.65)

Table 3. Weighted mean AUC and 95% CI results for upregulated and downregulated subsets of gene signature using the ssGSEA, GSVA, and Singscore (bidirectional version). Color-coded for AUC values that were 0.05 greater (red) than the original model and were 0.05 less (blue) than the original model . (*: p <= 0.01, **: p <= 0.001, ***: p <= 0.0001 derived from Wilcoxon signed-rank test).

Signature	TBSignatureProfiler (Original Model)	TBSignatureProfiler (ssGSEA: upregulated)	TBSignatureProfiler (ssGSEA: downregulated)	TBSignatureProfiler (GSVA: upregulated)	TBSignatureProfiler (GSVA: downregulated)	TBSignatureProfiler (Singscore)
Verhagen_10	0.61 (0.57-0.66)	0.55 (0.54-0.58)	0.57 (0.55-0.62)	0.56 (0.53-0.60)	0.62 (0.58-0.67)	0.56 (0.54-0.59)
Sambarey_HIV_10	0.83 (0.76-0.87)	0.82 (0.78-0.85)	0.68 (0.64-0.73)	0.82 (0.78-0.85)	0.71 (0.65-0.76)	0.67* (0.62-0.74)
Maertzdorf_15	0.82 (0.79-0.85)	0.71* (0.67-0.76)	0.85 (0.81-0.88)	0.71** (0.68-0.75)	0.84 (0.80-0.88)	0.80 (0.77-0.84)
Leong_24	0.72 (0.67-0.78)	0.80 (0.76-0.85)	0.73 (0.69-0.77)	0.76 (0.71-0.80)	0.73 (0.69-0.77)	0.80 (0.76-0.84)
Kaforou_27	0.81 (0.77-0.85)	0.84 (0.81-0.88)	0.72*** (0.68-0.76)	0.83 (0.80-0.87)	0.71*** (0.67-0.75)	0.82 (0.78-0.86)
Anderson_42	0.78 (0.73-0.83)	0.82 (0.78-0.86)	0.73* (0.69-0.78)	0.81 (0.78-0.84)	0.72* (0.68-0.76)	0.81 (0.77-0.85)
Kaforou_OD_44	0.76 (0.69-0.81)	0.81 (0.75-0.84)	0.65 (0.59-0.71)	0.80(0.74-0.84)	0.64 (0.59-0.70)	0.74 (0.67-0.80)
Anderson_OD_51	0.71 (0.64-0.78)	0.75 (0.70-0.80)	0.73 (0.70-0.76)	0.81 (0.78-0.84)	0.77 (0.71-0.82)	0.65* (0.62-0.70)
Kaforou_OD_53	0.83 (0.78-0.87)	0.85 (0.81-0.88)	0.75*** (0.70-0.80)	0.84 (0.81-0.87)	0.76*** (0.70-0.80)	0.82 (0.78-0.86)
Berry_OD_86	0.69 (0.66-0.72)	0.78*** (0.75-0.82)	0.63 (0.60-0.68)	0.80*** (0.76-0.84)	0.70 (0.66-0.75)	0.78** (0.74-0.82)
Bloom_OD_144	0.70 (0.66-0.74)	0.78 (0.74-0.83)	0.64 (0.60-0.68)	0.78 (0.73-0.83)	0.64*** (0.61-0.68)	0.77 (0.73-0.81)
Berry_393	0.70 (0.66-0.74)	0.80* (0.76-0.85)	0.74 (0.70-0.79)	0.79* (0.76-0.84)	0.74 (0.70-0.79)	0.79** (0.75-0.84)
Leong_RISK_29	0.68 (0.65-0.73)	0.72 (0.69-0.77)	0.69 (0.64-0.75)	0.76 (0.72-0.80)	0.71 (0.66-0.75)	0.73** (0.70-0.77)

Figure 2. Differences of the weighted mean AUC values between the original model versus gene set scoring methods. Each grid showed the difference of weighted mean AUC value between the use of the corresponding gene set scoring methods (ssGSEA, GSVA, PLAGE, and Singscore) and the use of original models. The results from the original model was used as the baseline. For all 19 TB gene signatures, the weighted mean AUC results computed by ssGSEA, Singscore, GSVA, and Zscore were statistically equivalent from the results given by the original model **(A)**. The weighted mean AUC results computed by ssGSEA and GSVA for the upregulated subsets of the gene signatures, Singscore (bidirectional scoring), and GSVA for the downregulated subsets of the gene signatures were statistically equivalent from the results given by the original model **(B)**. Red: the weighted mean AUC for gene scoring method outperformed the original model. Blue: the weighted mean AUC for gene scoring method underperformed the original model.
*: p-value < 0.05 derived from the Wilcoxon signed-rank test
**: p-value < 0.01 derived from Wilcoxon signed-rank test

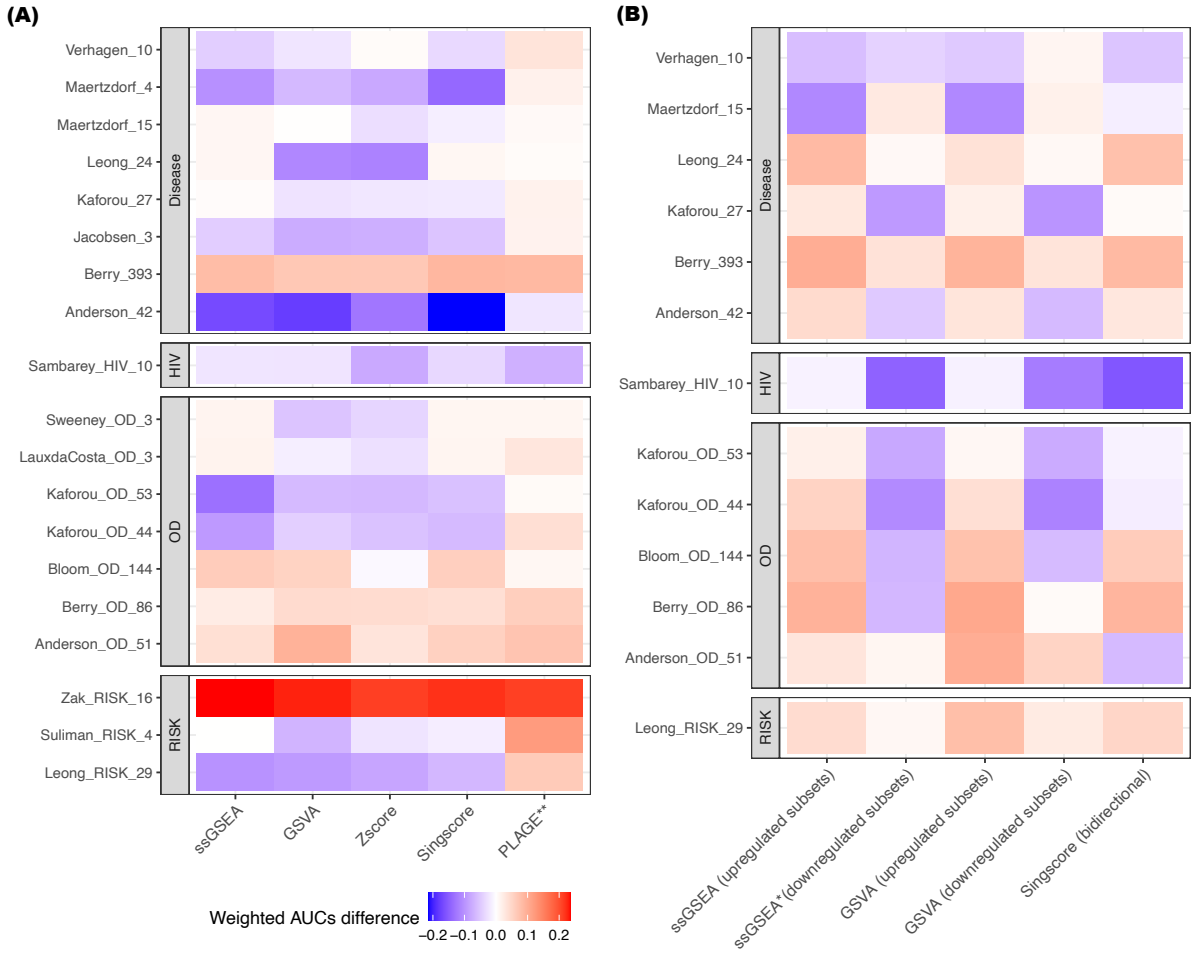

Supplementary Table 1. Summary of AUC and 95% CI results from gene signature's discovery/training study. The original publication section presented the AUC and 95% CI for each signature from their publication. The Warsinske et al. subsection showed the results that have been re-evaluated using the original models functionality that had been implemented in the TBSignatureProfiler, and the ssGSEA section presented the performance of each gene signature using ssGSEA from TBSignatureProfiler (Courtesy to Warsinske et al. work; ATB: active tuberculosis).

Signature	Clinical Comparison	Dataset Compared	Original Publication	Warsinske et al.	TBSignatureProfiler	
			AUC (95% CI)	AUC (95% CI)	AUC (95% CI) Warsinske et al.	AUC (95%CI) ssGSEA
Sweeney_OD_3	ATB vs. HCs	GSE19491✧	0.96 (0.94 - 0.98)	0.96 (0.94 - 0.98)	0.95 (0.91 - 0.99)	0.96 (0.91 - 0.99)
		GSE42834✧	1.00 (1.00-1.00)	1.00 (1.00-1.00)	1.00 (1.00 - 1.00)	0.92 (0.83 - 0.98)
	ATB vs. LTBI	GSE19491✧	0.93 (0.91 - 0.95)	0.93 (0.91-0.95)	0.92 (0.87 - 0.97)	0.93 (0.87 - 0.97)
		GSE37250	0.93 (0.91 - 0.94)	0.93 (0.91-0.94)	0.93 (0.90 - 0.95)	0.90 (0.86 - 0.93)
	ATB vs. OD	GSE19491✧	0.92 (0.89 - 0.94)	0.92 (0.89-0.94)	0.90 (0.84 - 0.95)	0.92 (0.88 - 0.97)
		GSE37250	0.87 (0.85 - 0.89)	0.87 (0.85-0.89)	0.87 (0.83 - 0.91)	0.83 (0.78 - 0.87)
		GSE42834✧	0.84 (0.80 - 0.88)	0.84 (0.80-0.88)	0.84 (0.79 - 0.90)	0.78 (0.67 - 0.85)
Jacobsen_3	ATB vs. LTBI	GSE19491✧	N/A	0.93 (0.91-0.95)	0.93 (0.88 - 0.97)	0.79 (0.71 - 0.86)
LauxdaCosta_OD_3	ATB vs. OD	GSE42834✧	0.95* (0.88-1.00*)	1.00 (1.00-1.00)	1.00 (1.00-1.00)	0.82 (0.76 - 0.88)
Maertzdorf_4	ATB vs. HCs	GSE74092	0.98 (0.96 - 1.00)	0.99 (0.99-1.00)	1.00 (1.00-1.00)	0.71 (0.64 - 0.79)
Sambarey_HIV_10	ATB vs. (LTBI & HCs & OD)	GSE37250*	N/A	0.89 (0.87-0.91)	0.89 (0.85 - 0.91)	0.79 (0.75 - 0.82)
Verhagen_10	ATB vs. (LTBI & HCs)	GSE41055	N/A	1.00 (1.00-1.00)	1.00 (1.00-1.00)	0.85 (0.66 - 0.97)
Maertzdorf_15	ATB vs. HC	GSE74092	0.99 (0.97 - 1.00)	1.00 (1.00-1.00)	1.00 (1.00 - 1.00)	0.95 (0.92 - 0.97)
Leong_24	ATB vs. LTBI	GSE101705	0.98 (0.98 - 0.98)	1.00 (1.00-1.00)	1.00 (1.00 - 1.00)	0.95 (0.87 - 1.00)
Kaforou_27	ATB vs. LTBI	GSE19491✧	0.98 (0.95 - 1.00)	0.95 (0.93-0.97)	0.96 (0.92 - 0.99)	0.95 (0.90 - 0.98)
Anderson_42	ATB vs. LTBI	GSE39940	0.98 (0.95 - 1.00)	0.97 (0.96-0.98)	0.98 (0.95 - 0.99)	0.93 (0.88 - 0.96)
Kaforou_OD_44	ATB vs. OD	GSE19491✧	0.95 (0.89 - 0.99)	0.91 (0.89-0.94)	0.93 (0.90 - 0.96)	0.69 (0.60 - 0.77)
Anderson_OD_51	ATB vs. OD	GSE39940	0.86 (0.77 - 0.94)	0.89 (0.87-0.91)	0.90 (0.87 - 0.94)	0.80 (0.75 - 0.85)
Kaforou_OD_53	ATB vs. (LTBI & HCs & OD)	GSE19491✧	N/A	0.92 (0.89-0.94)	0.92 (0.88 - 0.96)	0.71 (0.63 - 0.77)

Supplementary Table 1 (Continued)

Signature	Clinical Comparison	Dataset Compared	Original Publication	Warsinske et al.	TBSignatureProfiler	
			AUC (95% CI)	AUC (95% CI)	AUC (95% CI) Warsinske et al.	AUC (95%CI) ssGSEA
Berry_OD_86	ATB vs. LTBI	GSE19491✧	N/A	0.97 (0.96-0.99)	0.96 (0.92 - 0.98)	0.90 (0.85 - 0.95)
	ATB vs. HCs	GSE19491✧	N/A	1.00 (1.00-1.00)	0.99 (0.98 - 1.00)	0.89 (0.84 - 0.94)
Bloom_OD_144	ATB vs. (OD & HCs)	GSE42834✧	0.91 (Not available)	0.99 (0.98-1.00)	0.97 (0.94 - 1.00)	0.80 (0.71 - 0.87)
Berry_393	ATB vs. LTBI	GSE19491✧	N/A	0.97 (0.96-0.99)	0.96 (0.93 - 0.99)	0.94 (0.89 - 0.97)
	ATB vs. HCs	GSE19491✧	N/A	0.99 (0.98-1.00)	0.99 (0.97 - 1.00)	0.95 (0.91 - 0.98)
Leong_RISK_29	Progressor vs. Non-progressor	GSE79362 (Baseline)	N/A	N/A	0.96 (0.93 - 0.99)	0.56 (0.51 - 0.69)
Zak_RISK_16	Progressor vs. Non-progressor	GSE79362 (Total Time Period)	0.74 (0.73 - 0.76)	N/A	0.72 (0.61 - 0.82)	0.77 (0.62 - 0.87)
Suliman_RISK_4 (Site-Specific)	Progressor vs. Non-progressor	GSE94438	0.67 (0.57-0.77)	N/A	0.71 (0.65 - 0.77)	0.61 (0.55 - 0.67)

* Original training studies were not available for the signatures; ✧ Superseries of multiple datasets

Supplementary Figure 1. The distribution of AUC values for 19 TB gene signatures across 24 studies using ssGSEA **(A)**, GSVA **(B)**, PLAGE **(C)**, Zscore **(D)**, and Singscore unidirectional version **(E)**. Datasets had the same order as those from Figure 1.

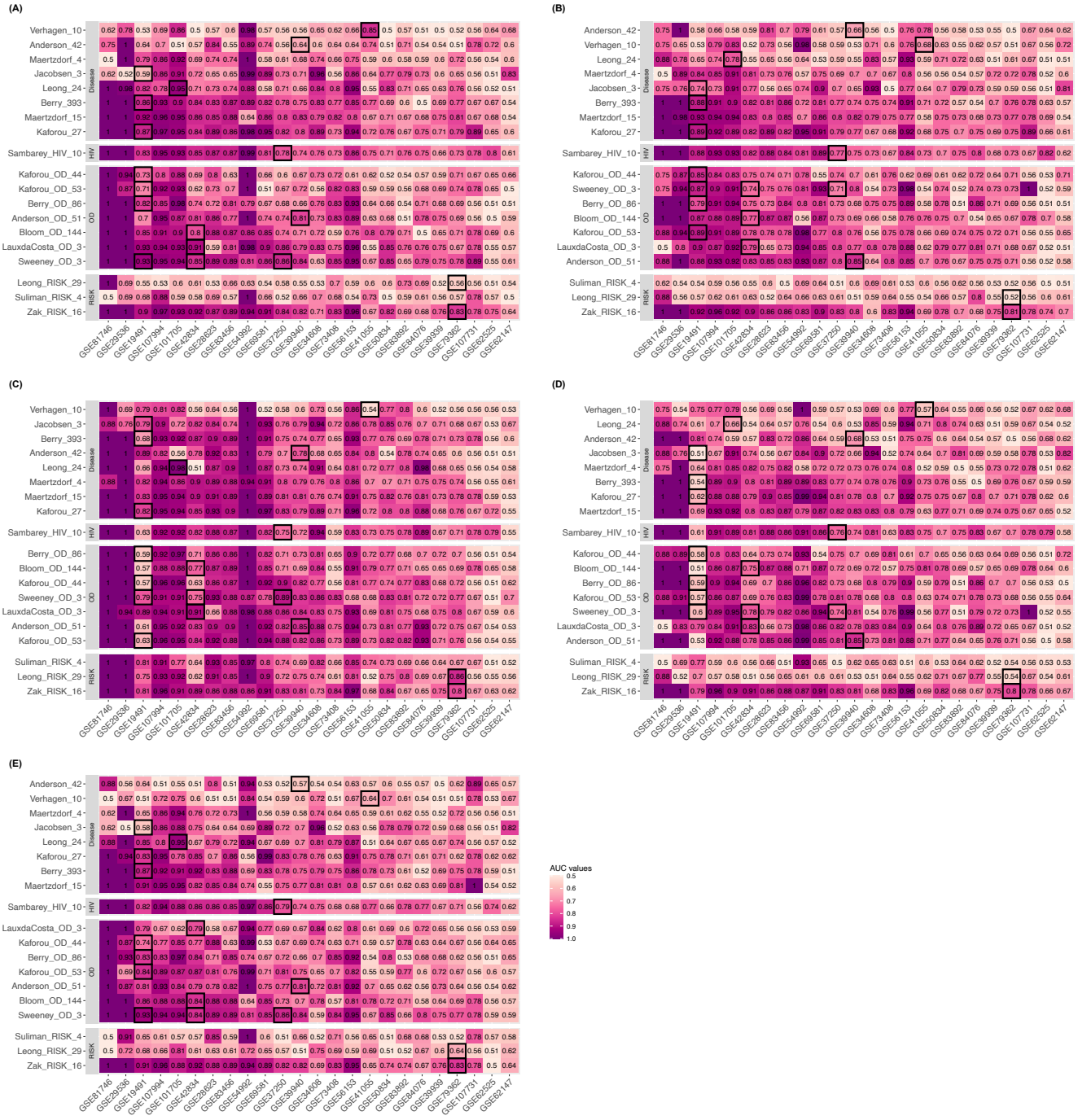

Supplementary Figure 2. The distribution of AUC values for **upregulated and downregulated subsets** of 13 TB gene signatures across 24 studies using ssGSEA **(A)**, GSVA **(B)**, and Singscore bidirectional version **(C)**. Datasets had the same order as those from Figure 1.

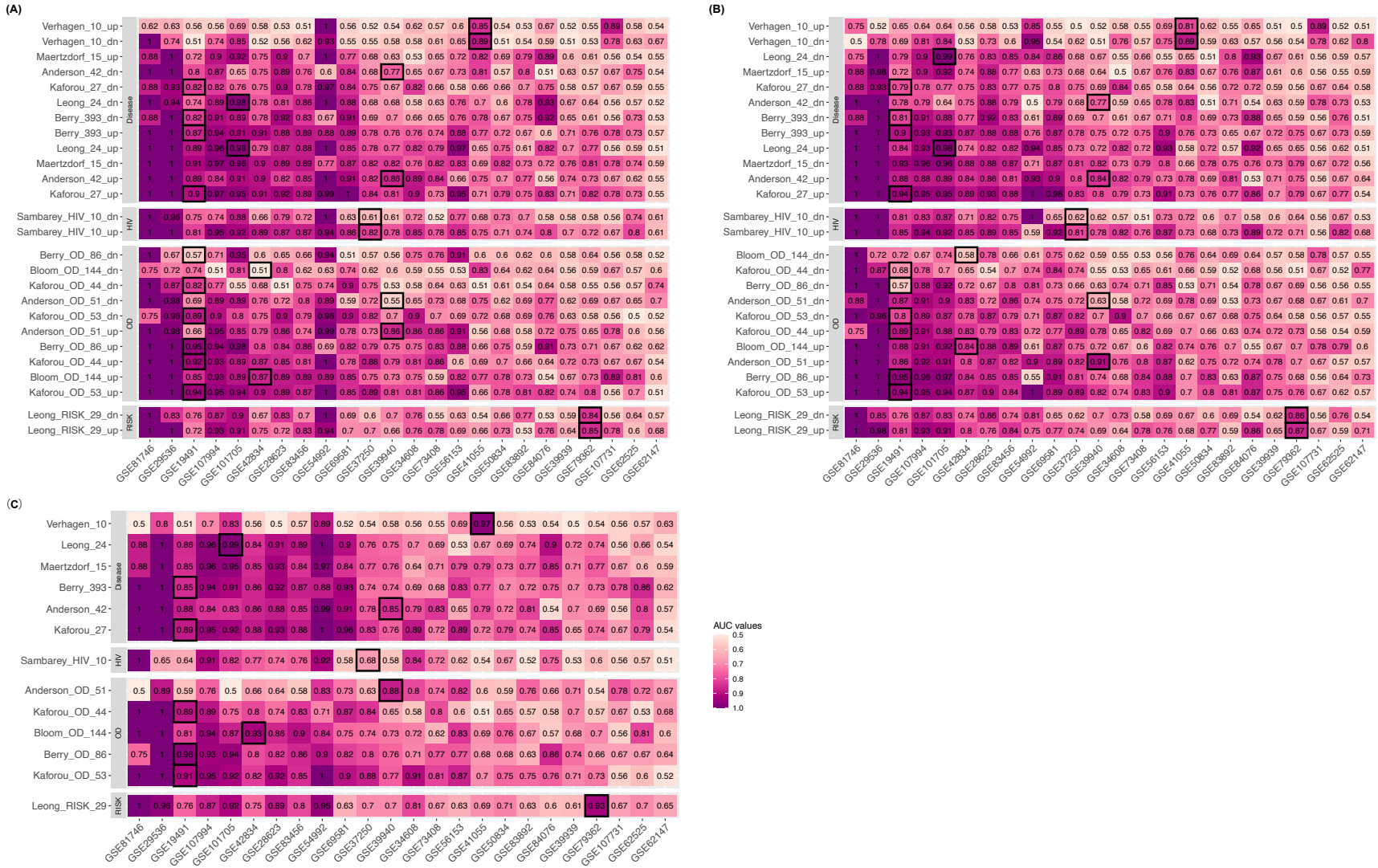

Supplementary Figure 3. The distribution of AUC values for TB gene signatures across 24 studies using the original models and gene set scoring methods in the form of ridge plot. Gene signatures were ordered based on the median AUCs given by the original models. **(A)** Comparison of AUC distributions given by ssGSEA (evaluated on the upregulated subsets of the gene signatures), PLAGE, and the original models. **(B)** Comparison of AUC distributions given by five gene set scoring methods (ssGSEA, PLAGE, GSVA, Singscore, Zscore) and the original models. **(C)** Comparison of AUC distributions given by ssGSEA (evaluated on the upregulated and downregulated subsets of gene signatures), GSVA (evaluated on the upregulated and downregulated subsets of gene signatures), and the original models.

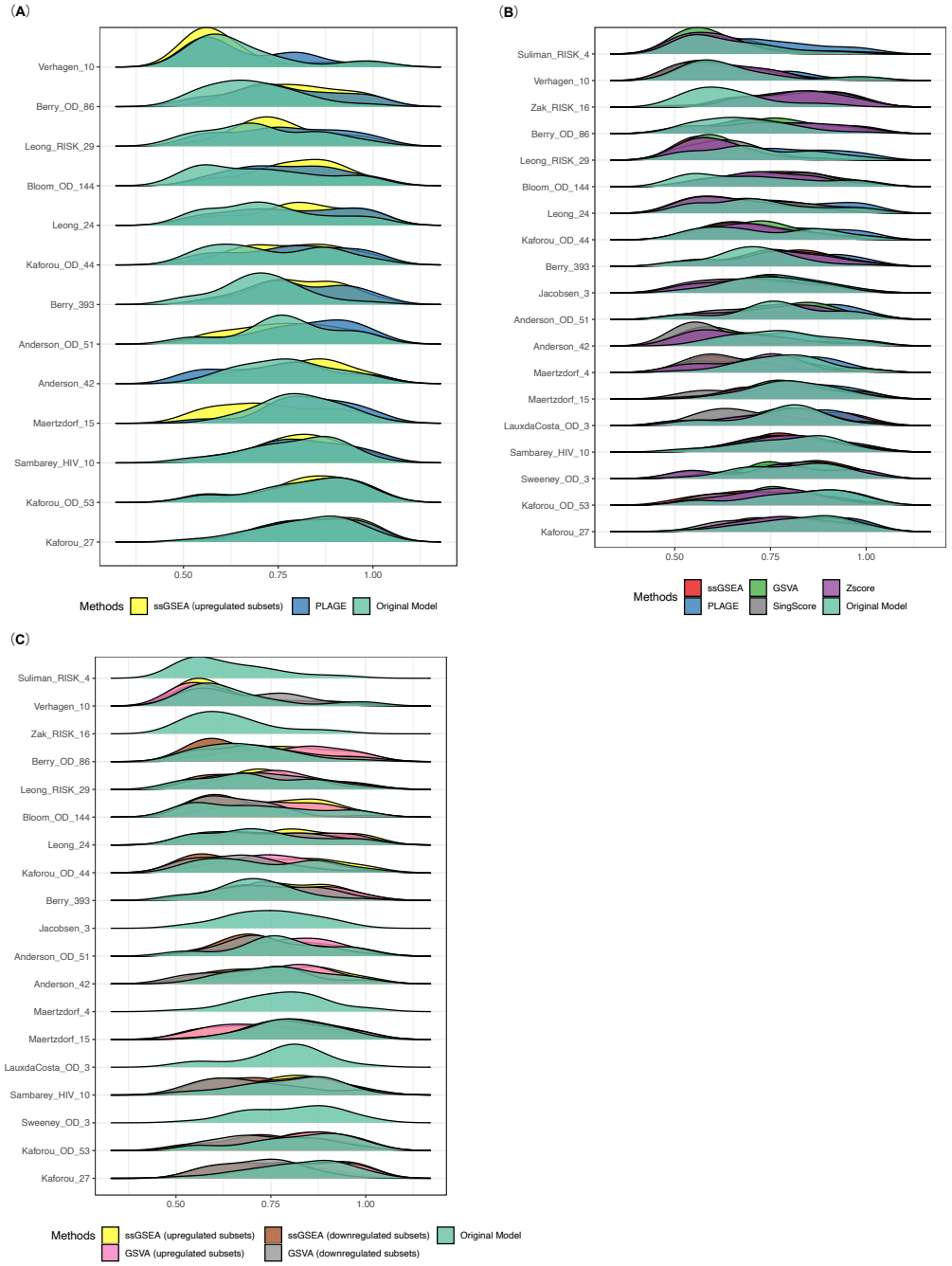

Supplementary Figure 4. Spearman's rank correlation versus AUC difference for studies with sample size larger than 40 and computed AUC values greater than 0.8 based on the results given by original models and ssGSEA **(A)**, original models and PLAGE **(B)**, original models and GSVA **(C)**, original models and Zscore **(D)**, original models and Singscore (unidirectional version) **(E)**. Overlapping points indicate the same dataset(s).
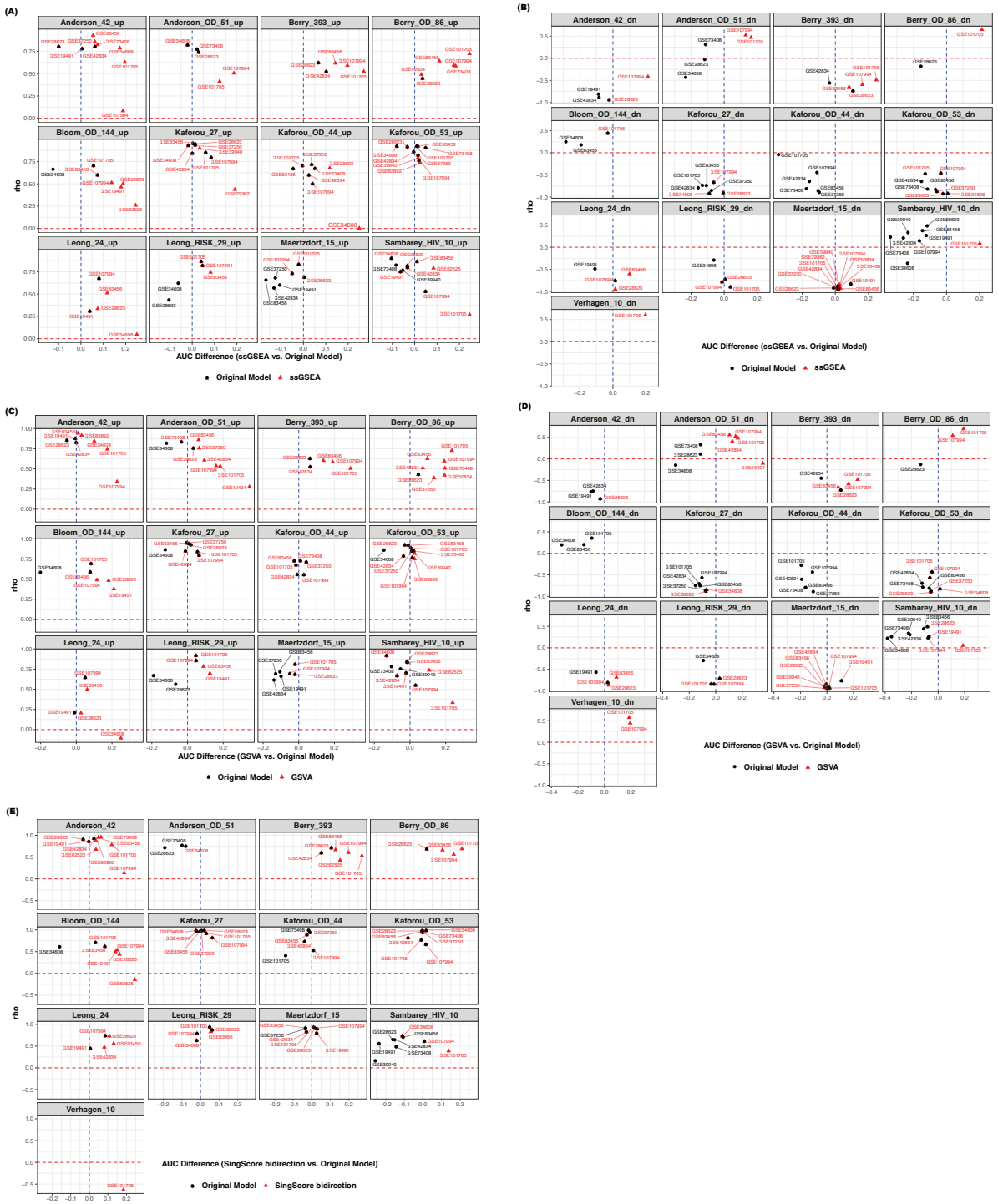
Supplementary Figure 5. Spearman's rank correlation versus AUC difference for studies with sample size larger than 40 and computed AUC greater than 0.8 based on results given by original models and ssGSEA (evaluated with upregulated subsets) **(A)**, original models and ssGSEA (evaluated with downregulated subsets) **(B)**, original models and GSVA (evaluated with upregulated subsets) **(C)**, original models and GSVA (evaluated with downregulated subsets) **(D)**, original models and Singscore (bidirectional version) **(E)**. Overlapping points indicate the same dataset(s).